



High cycle tensile fatigue of unidirectional fiberglass composite tested at high frequency
by Richard Francis Creed, Jr

A thesis submitted in partial fulfillment of the requirements for the degree of Master of Science in
Chemical Engineering
Montana State University
© Copyright by Richard Francis Creed, Jr (1993)

Abstract:

This thesis is part of a more general study of high cycle fatigue resistance of composite materials for use in wind turbine blades. Wind turbine blades experience roughly 10^8 to 10^9 significant loading-unloading fatigue cycles in their 20 to 30 year lifetime. This number of fatigue cycles would require 100 to 1000 days for a single fatigue test using a typical test frequency of 10 Hz. (cycles per second). Frequency limitations with conventional composite fatigue tests derive from hysteretic heating and poor thermal conductivity. The objectives of this research were to develop a test method for unidirectional fiberglass composites which would allow testing at a frequency of up to 100 Hz, and to obtain tensile fatigue ($R=0.1$) data beyond 10^8 cycles.

Attempts were made to develop a very small specimen while maintaining the fundamental material properties in order to improve the heat transfer. By modelling the heat transfer in a finite element analysis, it was shown that the thin specimens used in this study should not generate significant heating. This was confirmed by surface temperature measurements. Stress distributions in the specimen tab area were also analyzed by finite element analysis.

Fatigue tests were run over a range of stresses and lifetimes out to 1.8×10^8 cycles at frequencies ranging from 30 to 100 Hz. The S/N data trend was consistent with standard coupon data tested at low frequency in the low to moderate cycle range. Direct comparisons of 75 and 10 Hz tests show a slightly longer average lifetime at 10 Hz. The high cycle data indicate a less-steep S/N trend at higher cycles than is commonly observed in low to moderate cycle data sets for fiberglass materials.

HIGH CYCLE TENSILE FATIGUE OF UNIDIRECTIONAL
FIBERGLASS COMPOSITE TESTED AT HIGH FREQUENCY

by

Richard Francis Creed, Jr.

A thesis submitted in partial fulfillment
of the requirements for the degree

of

Master of Science

in

Chemical Engineering

MONTANA STATE UNIVERSITY
Bozeman, Montana

March 1993

COPYRIGHT

by

Richard Francis Creed, Jr.

1993

All Rights Reserved

71378
C862

ii

APPROVAL

of a thesis submitted by

Richard Francis Creed, Jr.

This thesis has been read by each member of the thesis committee and has been found to be satisfactory regarding content, English usage, format, citations, bibliographic style, and consistency, and is ready for submission to the College of Graduate Studies.

3/26/93
Date

John T. Maden
Chairperson, Graduate Committee

Approved for the Major Department

3/26/93
Date

John T. Sears
Head, Major Department

Approved for the College of Graduate Studies

3/30/93
Date

R. Brown
Graduate Dean

STATEMENT OF PERMISSION TO USE

In presenting this thesis in partial fulfillment of the requirements for a master's degree at Montana State University, I agree that the Library shall make it available to borrowers under the rules of the Library.

If I have indicated my intention to copyright this thesis by including a copyright notice page, copying is allowable only for scholarly purposes, consistent with "fair use" as prescribed in the U.S. Copyright Law. Requests for permission for extended quotation from or reproduction of this thesis in whole or in parts may be granted only by the copyright holder.

Signature

Richard Reed J

Date

March 29, 1993

ACKNOWLEDGEMENTS

There are a few people to whom credit should be given for their help and assistance with this research. I would like to extend my thanks to the following people. To Dr. Mandell, for his guidance and ideas on how to make this research turn into something meaningful. To Jane Curtis and Monica Hoey for help in obtaining equipment for use on this project. To Lyman Fellows for his efforts to make all the little gadgets I needed to continue in this research. To Sandia National Laboratories and Phoenix Industries for their financial and material support of this research.

TABLE OF CONTENTS

	Page
1. INTRODUCTION.....	1
2. BACKGROUND.....	3
Review of General Composite Fatigue Testing...	3
Review of Windmill Composite Material Fatigue.	11
Effects of Frequency on Fatigue.....	14
3. EQUIPMENT AND MATERIALS.....	16
Test Facility.....	16
Materials.....	18
4. RESULTS AND DISCUSSION.....	23
Finite Element Analysis.....	23
Stress Versus Number of Cycles Results.....	36
Frequency Effect.....	45
5. CONCLUSIONS AND RECOMMENDATIONS.....	51
Conclusions.....	51
Recommendations.....	53
REFERENCES.....	55
APPENDICES.....	60
APPENDIX A - Specimen Development.....	61
APPENDIX B - Hysteresis.....	66
APPENDIX C - Grips for Instron 8511.....	72

LIST OF TABLES

Table	Page
1. Summary of Material Properties.....	23
2. Summary of Finite Element Analysis of Heat Transfer.....	34
3. Summary of Raw Data.....	45
4. Frequency Effect Data.....	46
5. Loss Factors for Unidirectional Fiberglass Composite.....	70

LIST OF FIGURES

Figure	Page
1. Photograph of Instron 8511.....	17
2. Photograph of Manville Star Rov 502 EA Unidirectional E-glass Roving.....	19
3. Schematic of Specimen Dimensions and Tapping.....	21
4. Boundary Conditions for FEA of Stress Concentration.....	25
5. Micrograph of Specimen and Tapping, End View.....	26
6. FEA Results Showing Mesh and Stress Concentration Near the Tab (Close Up).....	27
7. FEA Results Showing Stress Redistribution into the Tab Region.....	29
8. Boundary Conditions for FEA of Stress Concentration with no Epoxy Layer Next to the Sample.....	30
9. FEA Results Showing Higher Stress Concentration with No Epoxy Layer next to the Specimen.....	31
10. FEA Heat Transfer Results of Temperature Versus Normalized Distance for Progressively Thicker Specimens.....	33
11. FEA Heat Transfer Results Showing Heat Dissipation into the Tab Region.....	35
12. Normalized S/N Curve for High Frequency Fatigue Tests.....	37
13. Photograph of Typical Broken Specimens from Different Load Levels and Frequencies.....	38
14. Normalized S/N Curve Comparing High Frequency Data to Windmill Material Standard Coupon Data.....	40

LIST OF FIGURES - Continued

Figure	page
15. Normalized S/N Curve Comparing High Frequency Data to Well Aligned Standard Coupon Data.....	41
16. High Cycle Specimen Data with Points Fit to Power Law and Semi-Logarithmic Curves.....	43
17. Load Versus Time Plot for Specimen Running at 10 Hz.....	47
18. Load Versus Time Plot for Specimen Running at 75 Hz.....	48
19. Displacement Versus Time Plot for Specimen Running at 10 Hz.....	49
20. Displacement Versus Time Plot for Specimen Running 75 Hz.....	50
21. Photograph of Random Mat Polyester and Steel Tabbing Regime.....	64
22. Explanation of Hysteresis and the Loss Factor.....	68
23. Time Versus Strain Curve for Unidirectional GRP....	69
24. Schematic of Instron 8511 Grips.....	74
25. Photograph of Grips with Specimen Running.....	75

ABSTRACT

This thesis is part of a more general study of high cycle fatigue resistance of composite materials for use in wind turbine blades. Wind turbine blades experience roughly 10^8 to 10^9 significant loading-unloading fatigue cycles in their 20 to 30 year lifetime. This number of fatigue cycles would require 100 to 1000 days for a single fatigue test using a typical test frequency of 10 Hz (cycles per second). Frequency limitations with conventional composite fatigue tests derive from hysteretic heating and poor thermal conductivity. The objectives of this research were to develop a test method for unidirectional fiberglass composites which would allow testing at a frequency of up to 100 Hz, and to obtain tensile fatigue ($R=0.1$) data beyond 10^8 cycles.

Attempts were made to develop a very small specimen while maintaining the fundamental material properties in order to improve the heat transfer. By modelling the heat transfer in a finite element analysis, it was shown that the thin specimens used in this study should not generate significant heating. This was confirmed by surface temperature measurements. Stress distributions in the specimen tab area were also analyzed by finite element analysis.

Fatigue tests were run over a range of stresses and lifetimes out to 1.8×10^8 cycles at frequencies ranging from 30 to 100 Hz. The S/N data trend was consistent with standard coupon data tested at low frequency in the low to moderate cycle range. Direct comparisons of 75 and 10 Hz tests show a slightly longer average lifetime at 10 Hz. The high cycle data indicate a less-steep S/N trend at higher cycles than is commonly observed in low to moderate cycle data sets for fiberglass materials.

CHAPTER ONE

INTRODUCTION

Fatigue in windmill blade materials is an important design consideration which has been based on an inadequate data base to date. The primary reason fatigue is so important with windmill materials is that each time a blade passes the tower, there is a lull in the wind and the blade flexes. Since a windmill usually operates at between one and three revolutions per second, the materials in the blade may see thirty million significant fatigue cycles each year, and in the twenty to thirty year lifetime they may see between one hundred and nine hundred million cycles. Catastrophic service failures early in the expected lifetime were not uncommon with many earlier blade designs [1].

Much of the previous research done in the area of glass reinforced polymers (GRP) under fatigue loading was only carried out to moderate numbers of cycles. There is a clear need for fatigue data in the 10^8 to 10^9 cycle range experienced by blades over their 20 to 30 year lifetime. Existing fatigue test methods for fiberglass have been limited to the 10 to 20 Hz range because of hysteretic heating and poor thermal conductivity, which overheat the material [2]. At 10 Hz, 10^8 cycles in a single test would

take about 100 days, and is , therefore, impractical. The objectives of this study were to develop a test method for tensile fatigue of unidirectional fiberglass which would allow testing in the range of 100 Hz, and to obtain data beyond 10^8 cycles. The approach was to use a small enough volume of material so that heat could be rapidly dissipated, while still maintaining the behavior of larger volumes.

CHAPTER TWO

BACKGROUND

Review of General Composite Fatigue Testing

The basic principle behind any cycle dependent behavior is that nonconservative changes occur in internal nature or geometry due to the loading history. In general, this implies that some of the energy introduced into a system is not stored as strain energy, but dissipated as any number of possible events, such as crack formation, heat loss, stress-corrosion, etc. [3].

Many early investigators of the fatigue of composite materials experimented with polyester reinforced with chopped strand E-glass mat. Owen and Dukes [4] performed many cyclic tests on this material, and proposed several mechanisms for failure. The first damage mechanism was debonding, initially of the fibers lying normal to the tensile stress. The next mechanism was the initiation of cracking in resin rich areas. The third and final mechanism was fiber failure, and separation into two pieces. Each of these mechanisms occurred upon higher stress or increased cycles.

Many of the investigations into unidirectional fiberglass fatigue ended without testing beyond one million

cycles. Dharan [5] performed an investigation of unidirectional fiberglass and described the failure mechanisms in three regions. The first region was dominated by fiber catastrophic failure, and usually occurred up to two hundred cycles with a corresponding high stress. Region II was once again dominated by fiber failure, but the broken fibers were far enough apart that failure was not immediate. These breaks were initiated by cracks in the matrix emanating from the surface. At later stages of Region II, the crack was said to follow the along the interface between fiber and matrix. The third region, which was beyond one million cycles, had no fiber failures. Dharan concluded that the stress level was below that which would be required to propagate a crack since the glass fiber stress corrosion mechanism requires a minimum stress, below which the crack tip radius in glass increases. This increase in crack tip radius results in little further crack growth [6]. Dharan discontinued testing at two million cycles because of this hypothesis.

Defining failure in a fatigue test is somewhat ambiguous. Many researchers consider that the specimen has failed when there are two pieces; others define failure as when there has been a degradation of modulus, or stiffness, to a percentage of the original value [7,8,9]. In windmill applications, a loss of modulus above a particular value will allow the blade to have a much greater flex than

originally expected and may allow the blade to hit the tower.

Fundamental testing of fatigue in GRP has been concentrated on laminates made from different fabrics and matrices. Fabrics can be made from chopped strands with random orientation or axial fibers stitched together with organic thread. Different matrices would include primarily epoxies, vinylesters, and polyesters for windmill applications. With a majority of laminates there are fibers in multidirectional arrays, a large portion of which are in the primary loading direction. Fibers in the other directions are for loads in other directions, but are responsible for damage initiation with loading along the primary axis. Fibers in the transverse direction act as stress concentrations in the very brittle matrix material. This causes the matrix in these layers to crack, and eventually cause damage in the axial layers which, in turn, will fail at some point. With the failure criterion of loss of stiffness, however, the material may be considered failed when the transverse layers fail [6].

Owen and Dukes performed many tests on chopped strand mat impregnated with polyester resin. Upon static and fatigue testing, damage was apparent at only thirty per cent of the ultimate strength of the material. This damage was associated with fibers perpendicular to the loading direction, and was initiated at many points on the strands.

At a load of twenty percent of the ultimate strength, damage was found along the interface between fibers and matrix at only one thousand cycles. The laminate could be expected to survive at least one million cycles before breaking into two pieces even though damage had begun two orders of magnitude of cycles earlier [4].

The effect of matrix on the fatigue strength of a composite has been described by Broutman and Sahu [10]. They concluded that epoxies had the best properties for high cycle low stress fatigue, and phenolics had the best properties for short term high stress tests. Polyester matrix materials started out with properties between phenolic and epoxy, but dropped off rapidly. For long life tests, polyester had slightly lower properties than phenolics, but much lower than epoxide materials [10].

Determinations of residual (remaining) strength at different stages of fatigue lifetime were performed by Broutman and Sahu [10]. The strength of a GRP decreases with increasing cycles, although there is much associated scatter. The methodology for determining the decrease in residual strength was to initially determine the stress versus number of cycles (S/N) curve for crossplied prepreg laminate. Based on expected lifetimes, for particular load levels, specimens were fatigued to percentages of that lifetime and then broken. Plots of number of cycles versus residual strength for different fatigue load levels were

reported. At higher load levels the ultimate strength tends to drop off rapidly, but at low load levels the strength tends to remain almost constant. Unfortunately, the report does not show the strength of the low stress specimens at high cycles [10]. Similar work was done by Rotem [11] who developed a mathematical model for predicting residual strength from cumulative fatigue theory. Resulting calculations show that the degradation of residual strength only occurs near the end of the fatigue life. Experimental results from Rotem [11] and Broutman and Sahu [10] show that the model closely predicts actual behavior.

Reifsnider *et al* [3] reported extensive research with unidirectional carbon fiber/epoxy laminates with 0, 90, and ± 45 degree plies. By utilizing light microscopy and edge replications, characterization of damage processes within laminates has been possible. Initially, cracks occur in the matrix of the off-axis plies either in the matrix material, or more commonly, in the interface between fiber and matrix. This is commonly called interfacial debonding. These initial cracks form and meet axial plies and eventually begin to cause damage in these main load bearing plies. This damage comes in the form of broken fibers and delamination. At some point, the amount of damage in the laminate tends to level off for a period of time. This area is called the Characteristic Damage State (CDS). Up to this point, the amount of stress necessary to cause localized

cracking has been enough to cause cracks spaced far apart in a ply. At a transverse crack surface the stress in the axial (0°) direction is zero, building up to the overall applied stress some distance from the crack face.

Eventually, the stress or cycles will increase to a level high enough to cause another crack in the off axis ply. At some point, there will be a saturation level of cracks because the stress level between cracks will not be able to reach a high enough value to cause further cracking. This state is the Characteristic Damage State as described above. Further cycling beyond this point will cause delamination and fiber failure in the axial plies, eventually generating total separation [3].

One interesting characteristic of composite materials is the ability to withstand a large amount of damage without a significant loss of strength. In some cases where the specimen has a flaw such as a hole in the center or a notch in the edge, the strength of the composite actually goes up after some cycles have been put on the specimen. Such an example was reported by Stinchcomb and Bakis [12]. In the case where a static test is performed on a composite specimen with a round hole machined through the center, failure occurs on a line across the center of the hole. The hole generates a stress concentration and damage begins at its edges. When a fatigue test is run on a similar specimen, cracks and delaminations occur in the region

around the hole. This damage allows the stress to be redistributed around the hole, and consequently the specimen will have a higher static strength than one with no cycling. Although the static strength of the composite is improved with some damage from cyclic loading, the alteration of the stress field around the hole will eventually cause wear out of the specimen upon further cycling [12].

Much of the research covered thus far has considered matrix cracking as a primary concern in the fatigue of composite materials. Work by Mandell et al [13] has shown that the matrix has little effect on the fatigue sensitivity of fiber dominated GRP. When comparisons are made between the slope of maximum stress versus number of cycles (S/N) curves and corresponding single cycle strengths for different strength materials, fiber orientations, distribution of fibers, fiber length, and fiber content, the fatigue resistance seems to be insensitive to the listed factors. Typically, all types of glass fiber dominated composites, with the exception of woven fabric composites, tend to lose about ten percent of their initial strength per decade of cycles. This corresponds to a slope of negative one tenth on a normalized S/N curve for most E-glass reinforced composites [13].

Single strand tests were performed by Mandell et al both with and without matrix material, and the S/N curves for both were similar. This led to the conclusion that the

fatigue behavior derives primarily from the reinforcement [13]. This conclusion derives from a comparison of the ratio of ultimate strength of many composite materials to the slope of their S/N curves. The slope of an S/N curve usually fits a linearized semi-logarithmic curve of the form [14]:

$$\frac{S}{S_0} = 1 - b \cdot (\log N) \quad (1)$$

Where S is the maximum stress on each cycle and S_0 is the one-cycle (static) strength. This comparison was made for many different matrices and volume percent fibers, as well as for fibers alone, and always came out to be about $b=0.1$ [14].

Although the fibers provide the dominant factor in material properties as well as fatigue performance, other factors may play significant roles in the breakdown of the composite in fatigue. Several sources note a sudden drop in modulus with different fibers and matrices, mostly attributable to debonding of the fiber matrix interface and matrix cracking. A study of the flexural fatigue of unidirectional fiberglass by Shih and Ebert, run in stroke control, showed significant fiber/matrix cracking corresponding to a loss in stiffness. Since the tests were run in stroke control, any loss in stiffness results in a lower load on the specimen [15].

Review of Windmill Composite Material Fatigue

A great deal of research has been completed specifically for wind turbine applications of composites. The major concern, as has been stated previously, is the reduction in properties with continued cycling which has been the emphasis of a majority of the work.

One of the most complete studies was done by Bach [8]. Several types of tests were run including tension-tension ($R = 0.1$, where $R = \text{minimum stress}/\text{maximum stress}$), reverse loading ($R = -1.0$), and variable amplitude (WISPER, wind energy-specific load spectra) tests. Test specimens for the $R = 0.1$ tests were standard coupon sized specimens run at frequencies between 1 and 20 Hz and stresses between 35 and 65 percent of the ultimate strength of the unidirectional glass reinforced polyester. Conclusions from the tests were that a fatigue limit would only be reached in the range of fifteen percent of the ultimate strength and greater than one billion cycles. Another significant conclusion was that the data tended to follow a negative ten percent slope similar to that reported in other studies.

Appel and Olthoff [from Ref. 8] utilized this data to statistically arrive at a prediction for lifetime of composites. This prediction is a modification of that made by Mandell and includes the possibility of a fatigue limit (equation 2 [8]).

$$S_n = S_0 \left(1 - \left(0.15 \left(1 - \frac{\text{sign} S_{\min} * |S_{\min}|}{\text{sign} S_{\max} * |S_{\max}|} \right) + 0.08 \right) \log N \right) \quad (2)$$

Tabs on the specimens used by Bach were 50 mm by 25 mm by 1.5 mm and had an angle tapered toward the gauge section for the last 5 mm. The author noted that almost all the specimens began delamination at the point of contact with the tab which spread as failure was imminent [8].

Much of the work done on windmill materials has either been done with reverse loading of full blades or coupon sized specimens. Conclusions by Kensche and Kalkuhl [16] show that even in the reverse loading regime there appears to be no fatigue limit before 100 million cycles for either coupon tests or full scale tests. WISPER loading on spar beams indicated that local instabilities, such as buckling, are the cause of most failures. When these instabilities are constrained, a spar can withstand more than five hundred WISPER cycles equivalent to eighty years of service. This conclusion was based on maximum strain levels of 0.6 percent on the spar. These results imply that higher design limits are possible on large diameter blades, greater than 25 meters, and therefore lighter more economic blades can be utilized [17].

The European design criterion for blade certification has a limit of 0.3 percent strain in the tension zone and 0.2 percent strain in the compression zone. Much of the work done shows that these values are quite conservative and

blades could be made much lighter and have adequate lifetimes to those made presently. Design criteria are often developed from laboratory scale testing which shows a large decrease in stiffness shortly before failure. Fatigue failure of larger components may not have this noticeable stiffness decrease, and therefore, failure prediction requires some method of inspection [18].

Recent studies reported by Mandell *et al* [19] on high cycle fatigue of windmill blade materials have led to several conclusions. Uniaxially reinforced materials were found to have an S/N data trend falling below the 10 percent loss of static strength per decade of cycles at high stresses expected from previous studies. The trend followed by the data is a power law with exponent of about $m = 13.5$.

$$\frac{S}{S_0} = N^{-\left(\frac{1}{m}\right)} \quad (3)$$

Effects of specimen width were studied by a comparison of data for 1 and 2 in. wide specimens. The study reported similar lifetimes at similar stress levels for the different width coupons. Specimens used in testing usually are machined and, therefore, have free (cut) edges. To study the effects of free edges, standard size specimens machined from sheets of material were tested and compared to specimens molded 2 in. wide, with reinforcement wrapped around at the edges. The resulting S/N data trend showed little or no effect of the free edges. Comparisons of

specimens with similar reinforcement but different matrix materials (polyester or vinylester) revealed that the matrix has little effect in overall composite lifetime. However, vinylester composites tend to have slightly higher static strength [19].

Effects of Frequency on Fatigue

Effects of testing frequency on fatigue have been studied for many types of chopped strand fiber composites with the following areas of concern: hysteretic heating, rate of damage generation, and strain rate effects on the residual strength on the last cycle [20].

Hysteretic heating is the greatest problem with obtaining high cycle fatigue data for fiber reinforced plastics. The heat transfer within the plastic is very poor and even small amounts of strain energy absorbed in cycling can build up and cause the plastic to fail. To determine the amount of hysteresis for a particular stress level, one method is to find the loss factor (η), sometimes referred to as the tangent decrement. The loss factor can be arrived at experimentally with the use of a torsion pendulum and equation 4 [21]:

$$\eta = \frac{\ln \frac{A_n}{A_{n+1}}}{\pi} \quad (4)$$

where A_n and A_{n+1} are amplitudes of successive cycles [21].

Relating the loss factor to the amount of energy dissipated in one cycle is done with equation 5 [22]:

$$D_s = 2\pi Q \eta \quad (5)$$

where D_s is the strain energy at the maximum displacement and Q is the heat generation. Gibson [22] has shown that PPG SMC-65 has a constant loss factor over the frequency range from 10 to 1000 hertz and typically falls around 0.01.

Although frequency does not play a role in the loss factor, the amplitude of the input wave does. Kensche [17] has shown that η decreases nonlinearly with decreasing amplitude. The results show a drop of about a factor of two in the loss factor with a drop in amplitude of about twenty to thirty percent for many specimens.

Frequency effects other than from hysteretic heating are small. Glass fibers and polymeric matrices can show significant effects of constant load (static) fatigue, and it has been shown that time at maximum load causes much higher damage than the strain rate used in reaching that load [20,23]. However, fatigue behavior tends to be most influenced by the number of cycles not the frequency of cycling, particularly at high cycles [20,21].

CHAPTER THREE**EQUIPMENT AND MATERIALS**Test Facility

The procedure used for fatigue testing of E-glass unidirectionally reinforced polyester is similar to that of testing larger coupons, but on a smaller scale. Fatigue testing was done on a servohydraulic Instron Model 8511 with a load capacity of 2248 pounds force. The machine is controlled by an Instron Model 8500 controller and computer software. This low force machine is designed for high frequency testing, with low friction bearings, a hydraulic supply of 20 gallons per minute, a ten gallon per minute servovalve, and a system pressure of 3000 psi. Figure 1 is a photograph of the Instron 8511.

The specimens were clamped into the load train by grips developed in this study (see Figure 22 in Appendix C). Gripping force is provided by four screws tightened to 10 in.-lbf. torque. Force and displacement were measured by a load cell, -5000 to 5000 pounds force capacity, and an LVDT (linear variable displacement transducer) respectively. An oscilloscope was used to define waveform quality at different frequencies. Specimen surface temperature was measured with Omega Tempdaq liquid crystal paints.

All tests were run in load control with a constant sine

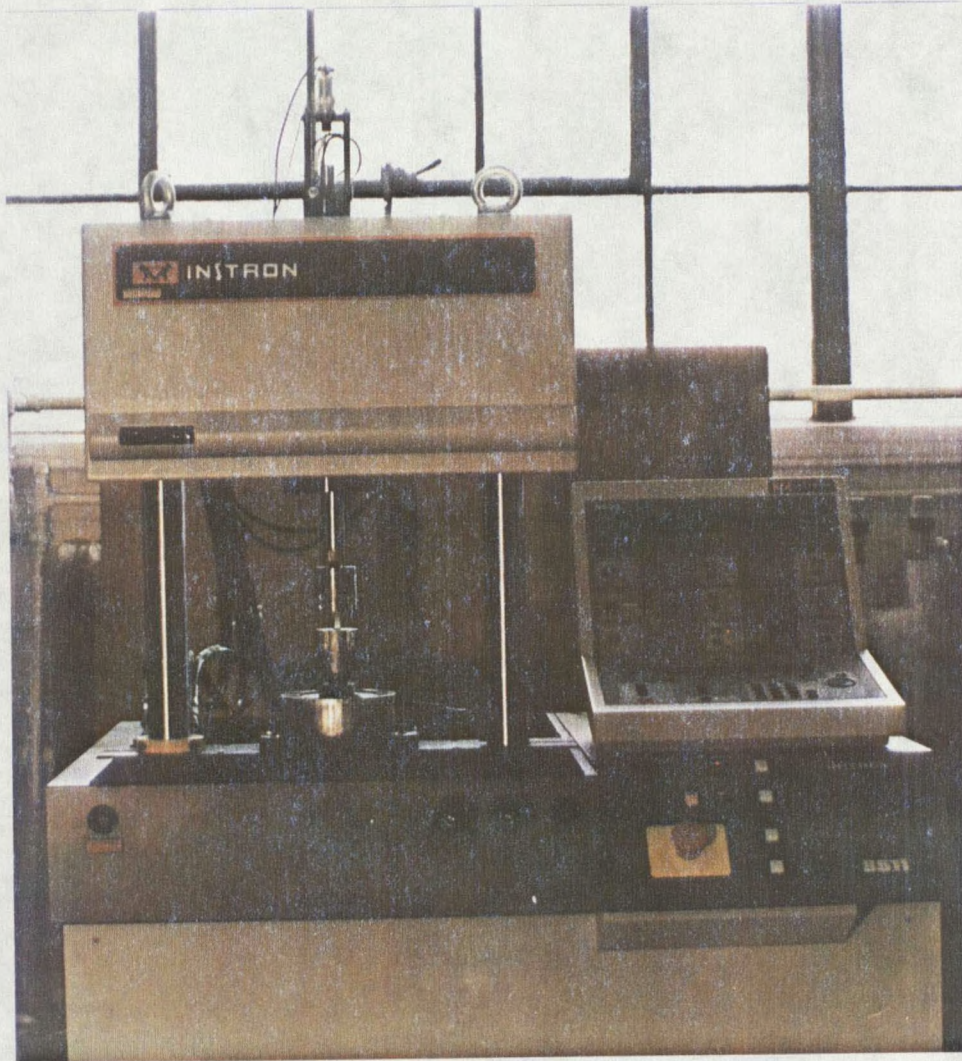


Figure 1. Photograph of Instron 8511.

wave input. The loading rate (maximum load/time to maximum load) was generally held constant between load levels by varying test frequency. Loading rate was varied somewhat because some testing frequencies gave poor waveforms and either speeding up or slowing down gave much better waveforms. Typical loading rates were between 8000 and 15000 pounds per second. The value chosen for single cycle tests was 4000 pounds per second, which was between one half and one third of the cyclic loading rate, in order to take many data points on a stress-strain curve. With higher loading rates, the stress-strain curve would be based on only a few points. This difference in loading rate should not significantly affect results [21].

All tests were conducted in ambient laboratory air. These ambient conditions are generally low humidity with temperatures between 65° and 80° F.

Materials

Raw materials were supplied by Phoenix Industries, and consisted of Manville Star Rove 502 EA glass fiber roving, one-quarter in. wide, and slow set orthophthalic polyester. Properties supplied by the manufacturer of the polyester are as follows: 0.68 msi modulus, 8.5 ksi ultimate tensile strength, and 1.10 g/cm³. Figure 2 is a photograph of the glass roving showing the inherent fiber misalignment. The specimens were made in the laboratory by applying enough

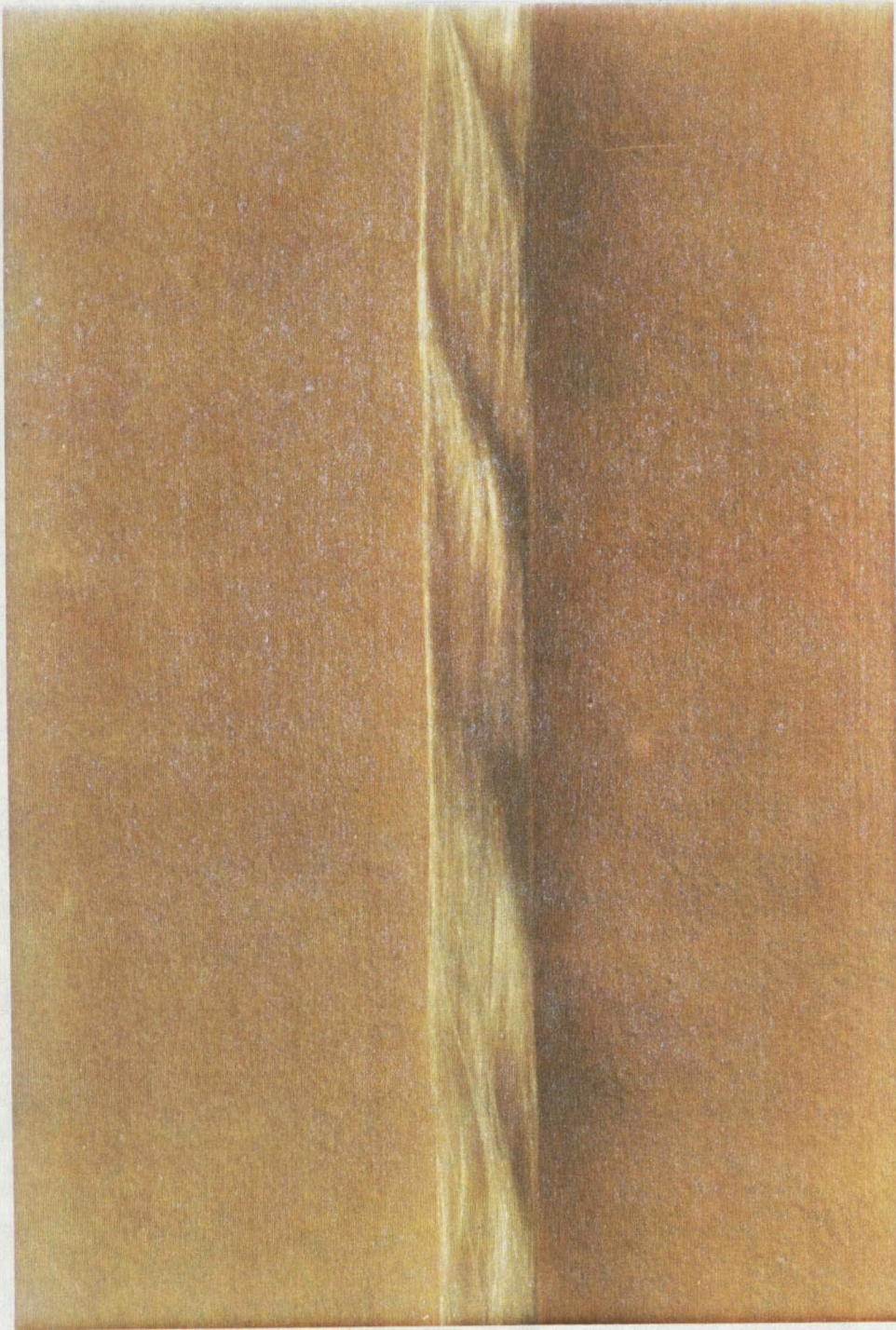
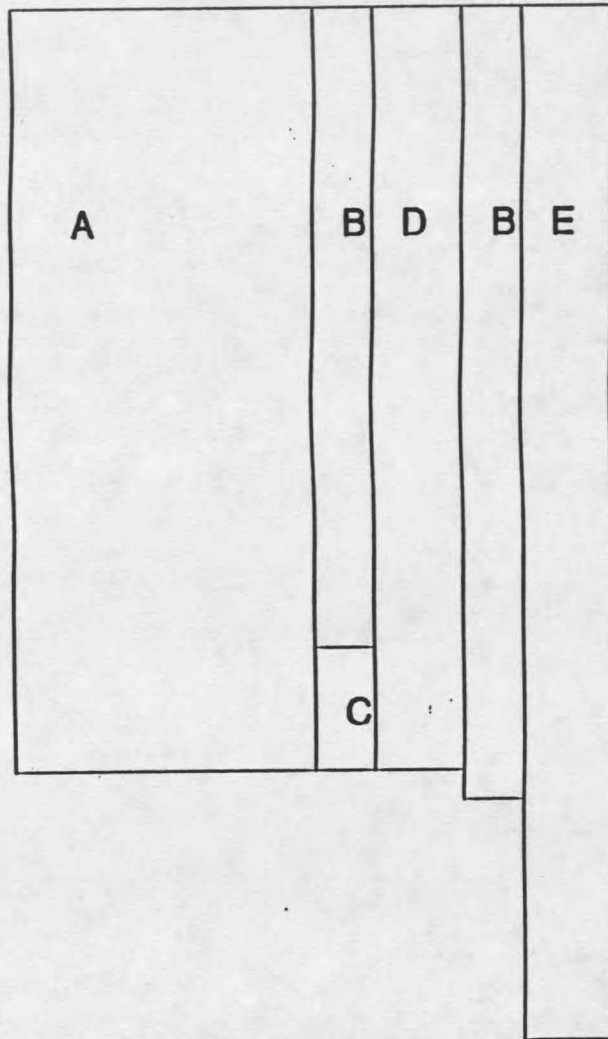


Figure 2. Photograph of Manville Star Rov 502 EA unidirectional E-glass roving.

tension to the glass fibers that they remain tight and impregnating them with the catalyzed polyester. Then, when the fiber/matrix combination became tacky, the composite was pressed between rubber sheets and cured for 24 hr. at 140° F. This gave a flat sample with parallel faces in the width direction. These samples, approximately 0.25 in. by 0.017 in. by 12 in., were then cut into 2.5 in. lengths. The fiber content of the specimens was between 45 % and 52 % by volume calculated from weight percent values and densities. The strength of the specimens was experimentally determined at $94,200 \pm 4100$ psi with a Young's modulus of 5 msi.

To prepare the test specimen tabs (Figure 3 shows an exaggerated cross section of tab area and dimensions of specimen), a single layer of 3M SP-250E unidirectional E-glass prepreg was cured into a flat sheet and cut into pieces 0.25 in. by 0.75 in. by 0.02 in., with the fibers in the long direction. These were used as the first layer of the tab. Each specimen had four of these prepreg pieces, one on both sides of both ends, bonded on with Hysol 9309.2 NA high toughness epoxy. The method of keeping the prepreg fibers aligned with the specimen fibers was to put the specimens between rubber sheets and apply roughly 0.5 psi over the entire surface. The prepreg pieces tend to slip out of alignment with other assembly methods. The last part of the tabbing procedure was to again use Hysol 9309.2 NA to bond on a relatively thick piece of 0/90 glass reinforced



- A) GRVE (0.0625 IN. THICK)
 - B) EPOXY (0.002 IN. THICK)
 - C) TEFLON FILM (0.002 IN. THICK)
 - D) SP250-E UNIDIRECTIONAL GLASS/EPOXY (0.02 IN THICK)
 - E) SPECIMEN(0.017 IN THICK)
- (EXAGGERATED THICKNESSES)

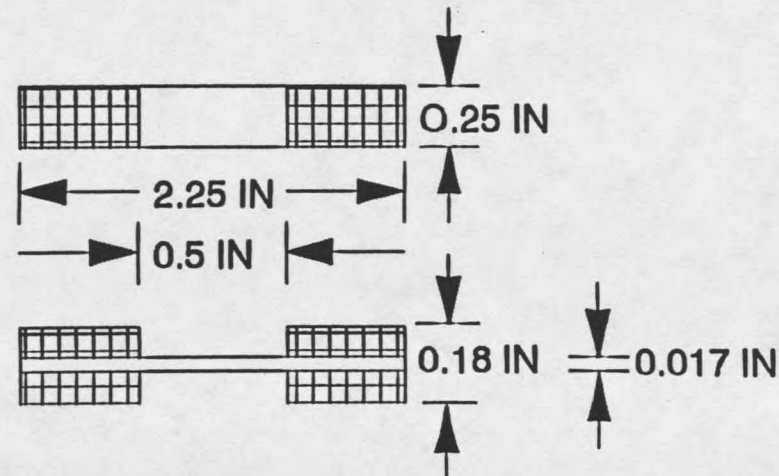


Figure 3. Schematic of tabbing for test specimen.

vinyl ester (GRVE) 0.0625 in. by 0.25 in. by 0.75 in. on both sides of each end (this is unpunched electrical vectorboard obtained from Plastifab inc.). Between the SP250-E and the GRVE, a 0.125 in. wide layer of teflon film was added on the gauge end of the tab (Figure 3). After each layer was added, a curing period of 24 hr. at 140° F. was necessary to cure the adhesive.

The specimen was then placed in the grips so that the top of each tab was flush with the grip. Alignment was achieved by marking the center of the specimen and lining this up with the vertical center lines on the grips. Some fiber misalignment is inherent in the material, causing waviness to the specimen, but care was taken to reduce misalignment to a minimum.

Several other tabbing arrangements were attempted, with generally poor results. These are discussed in Appendix A.

CHAPTER FOUR

RESULTS AND DISCUSSION

Finite Element Analysis

Modelling of the specimen for stress analysis and heat transfer was done with a commercial software package, COSMOS/M version 1.65. The elements used in both cases were plane two dimensional (plane2d) elements. These are four node, two dimensional linear displacement elements. The following material properties were used:

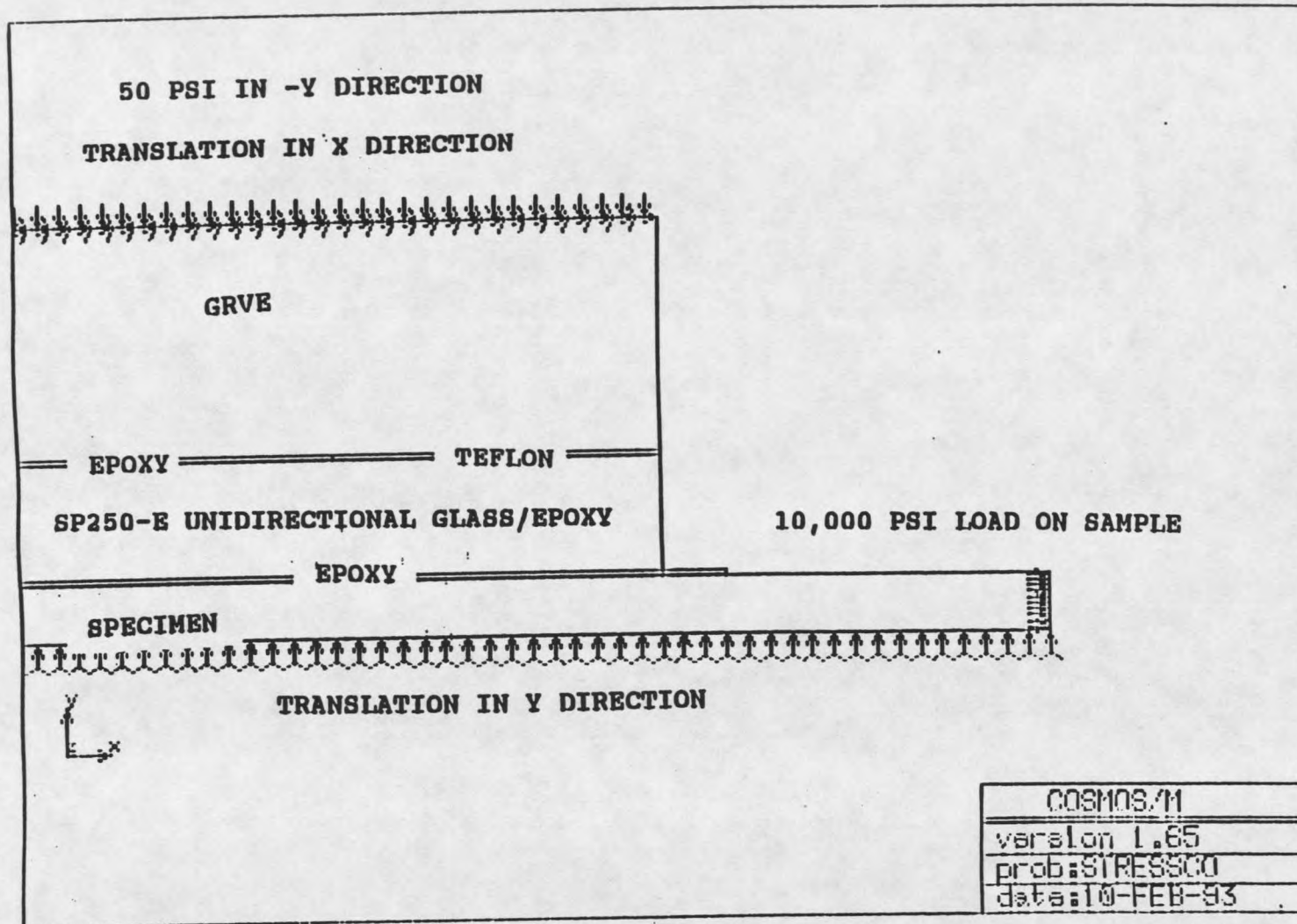
Table 1. Summary of Material Properties.

MATERIAL	E_L 10^6 psi	E_T 10^6 psi	ν_{LT}	G_{LT} 10^5	K_{ALL} $\frac{10^{-6} BTU}{in^2 * sec * ^\circ F}$
Specimen [24, *]	5.0	1.3	0.25	7.0	2.4 [25]
SP250E. [26]	6.0	1.5	0.25	8.5	1.5 [25]
0/90 Vinyl Ester [24]	1.5	1.5	0.3	6.0	1.5 [25]
Epoxy [27]	0.35	3.5	0.35	1.0	N/A
Teflon [27]	0.08	0.08	0.35	0.25	N/A

* Experimental results, E_L : Longitudinal Elastic Modulus;
 E_T : Transverse Elastic Modulus; ν_{LT} : Poison's Ratio;
 G_{LT} : Dynamic Modulus; K_{ALL} : Thermal Conductivity

Two types of analysis were necessary to qualify the specimen geometry. First, the specimen had to be analyzed for stress concentration near the tab. There is likely to be some stress concentration in the axial direction where the tab meets the specimen, and finite element analysis can show the approximate size and shape of the affected area. One quarter of the specimen was modelled utilizing symmetry boundary conditions on the specimen mid-length and mid-thickness. Other boundary conditions used in the model were translation in the Y-direction on the tab edge, a pressure of 50 psi on the tab, and a pressure of 10000 psi in the X-direction on the end of the specimen. Figure 4 shows the boundary conditions and the specimen geometry. The epoxy layer thickness was obtained from approximating the thinnest film between an average specimen and its tab, as can be seen in Figure 5.

The results from the analysis show a maximum stress about 0.001 in. (two fiber diameters) in from the edge at the point of contact with the tab material. Figure 6 is the output from Cosmos/m zoomed in on the point of interest, also showing the element mesh. The stress at this point is calculated at about 18 percent higher than the axial stress. However, this may be higher than the actual stress in the material because the specimen has discrete fiber and matrix regions which will tend to spread out the stress transfer. Discrete fibers and matrix could not reasonably be modelled



25

Figure 4. Boundary conditions for FEA of stress concentration.

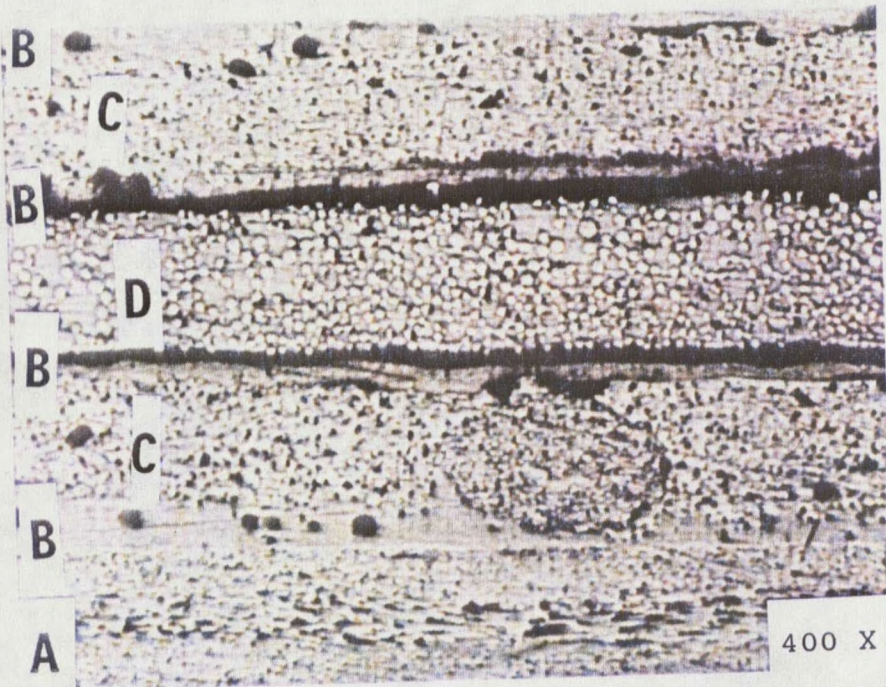


Figure 5. Micrograph of specimen and tabbing, end view, A is GRVE, B is epoxy, C is SP250E, and D is the specimen.

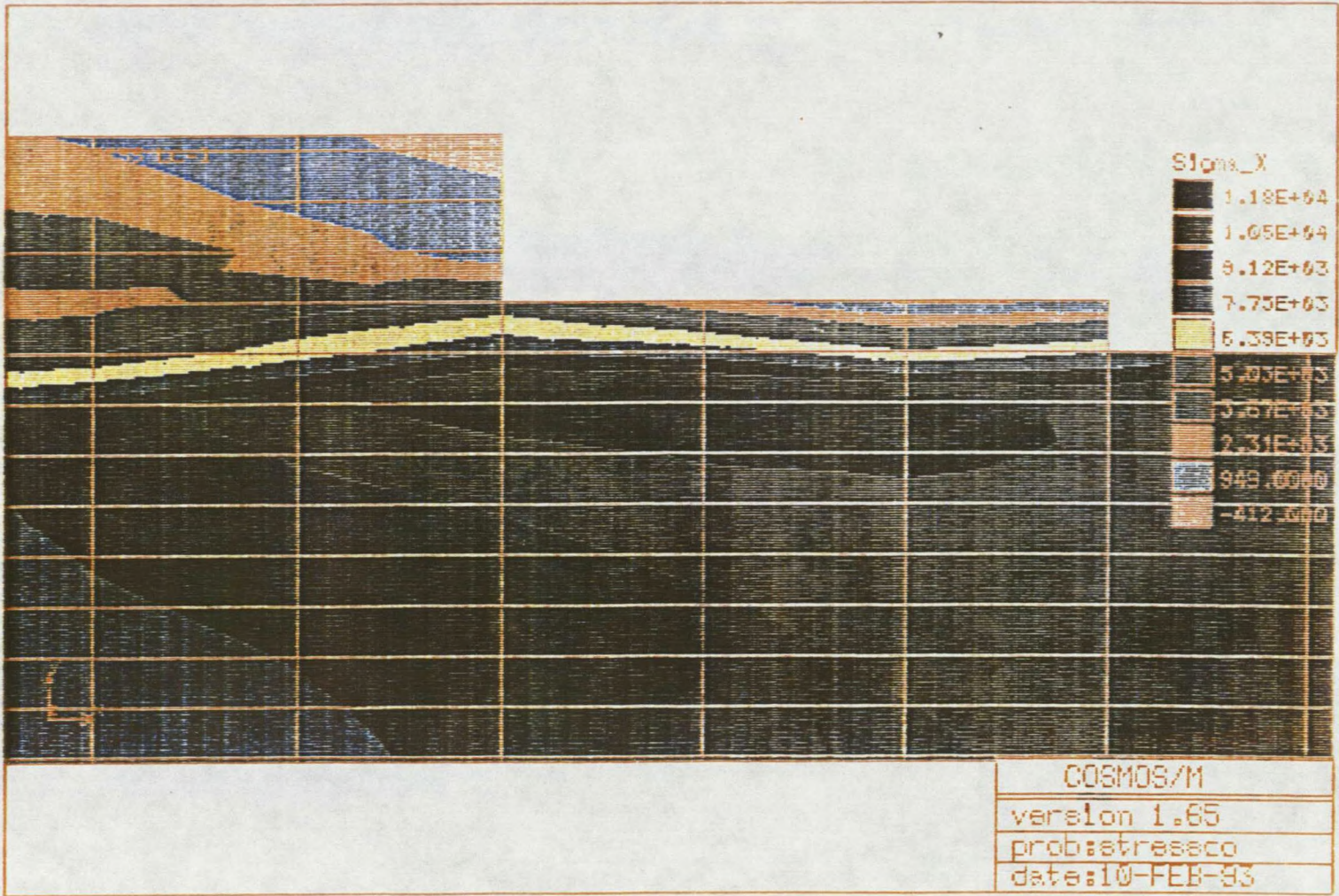


Figure 6. FEA results showing mesh and stress concentration near the tab (close up).

within the scope of this study. Figure 7 is of a larger portion of the specimen (with mesh), showing the stress dropping off inside the tab region. Some concentration of stress at the intersection of two materials is almost unavoidable. However, combined with the observation that specimens appear not to break in the tab region on every test (discussed later), the low level of stress concentration is considered to be acceptable.

One question about the validity of the FEA solution was whether the Teflon should be "bonded" to the surfaces around it. In order to determine if this had an impact, the same model was run with very low properties (10 percent of the original values) for the Teflon. This would closely simulate a free surface without problems of materials overlapping in the results. The stress concentration at the tab/specimen intersection came out to be exactly the same as the above model. Thus, the Teflon may not be essential to the tab arrangement.

For comparison, a model of the same tab arrangement was performed with the same boundary conditions, but with no fillet layer of epoxy at the surface of the specimen. The stress concentration is much higher in this case, sixty four percent higher than the applied stress as opposed to eighteen percent. Figure 8 shows the model geometry and the boundary conditions, and Figure 9 shows the stress concentration in the area of concern. This comparison shows

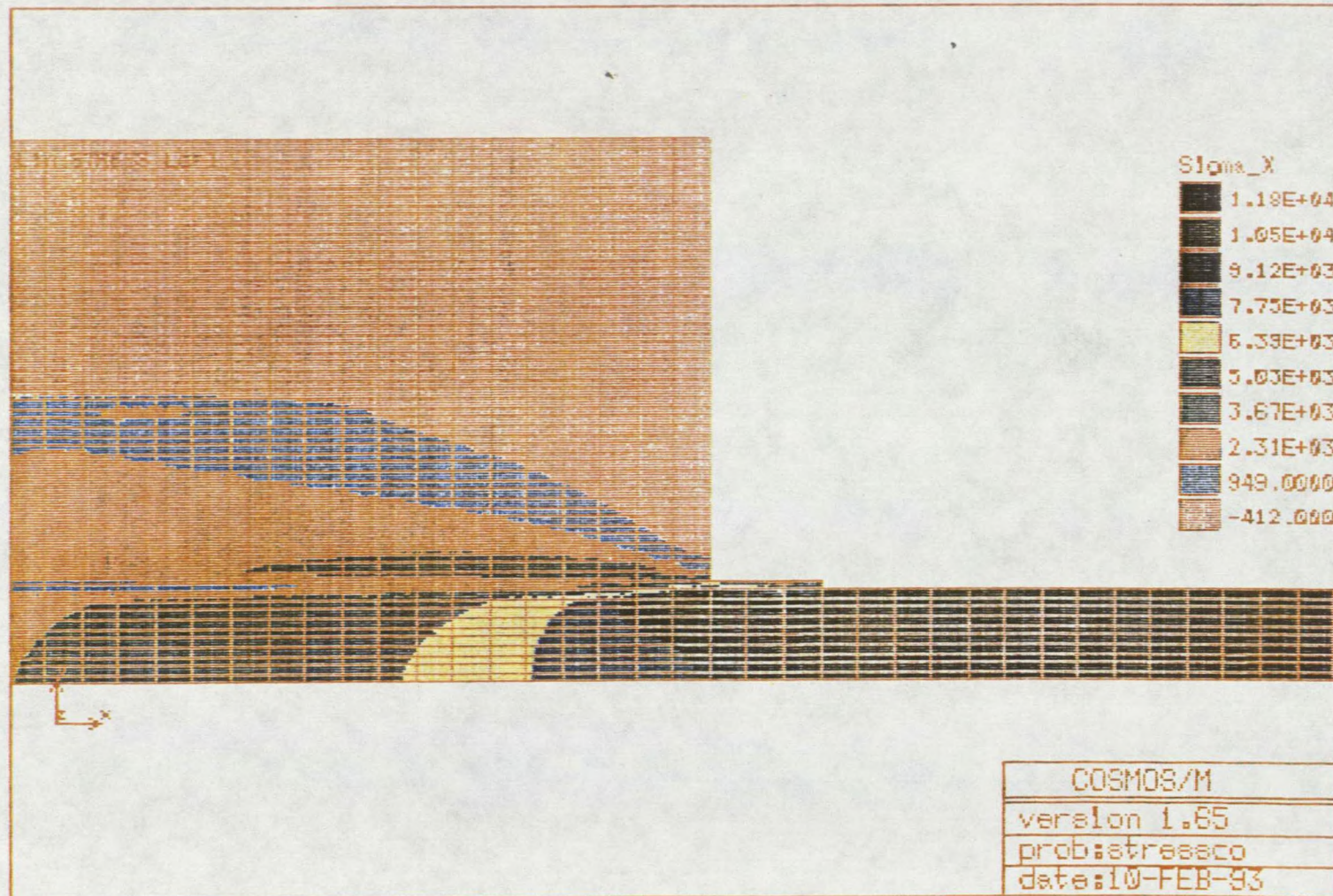


Figure 7. FEA results showing stress redistribution into the tab region.

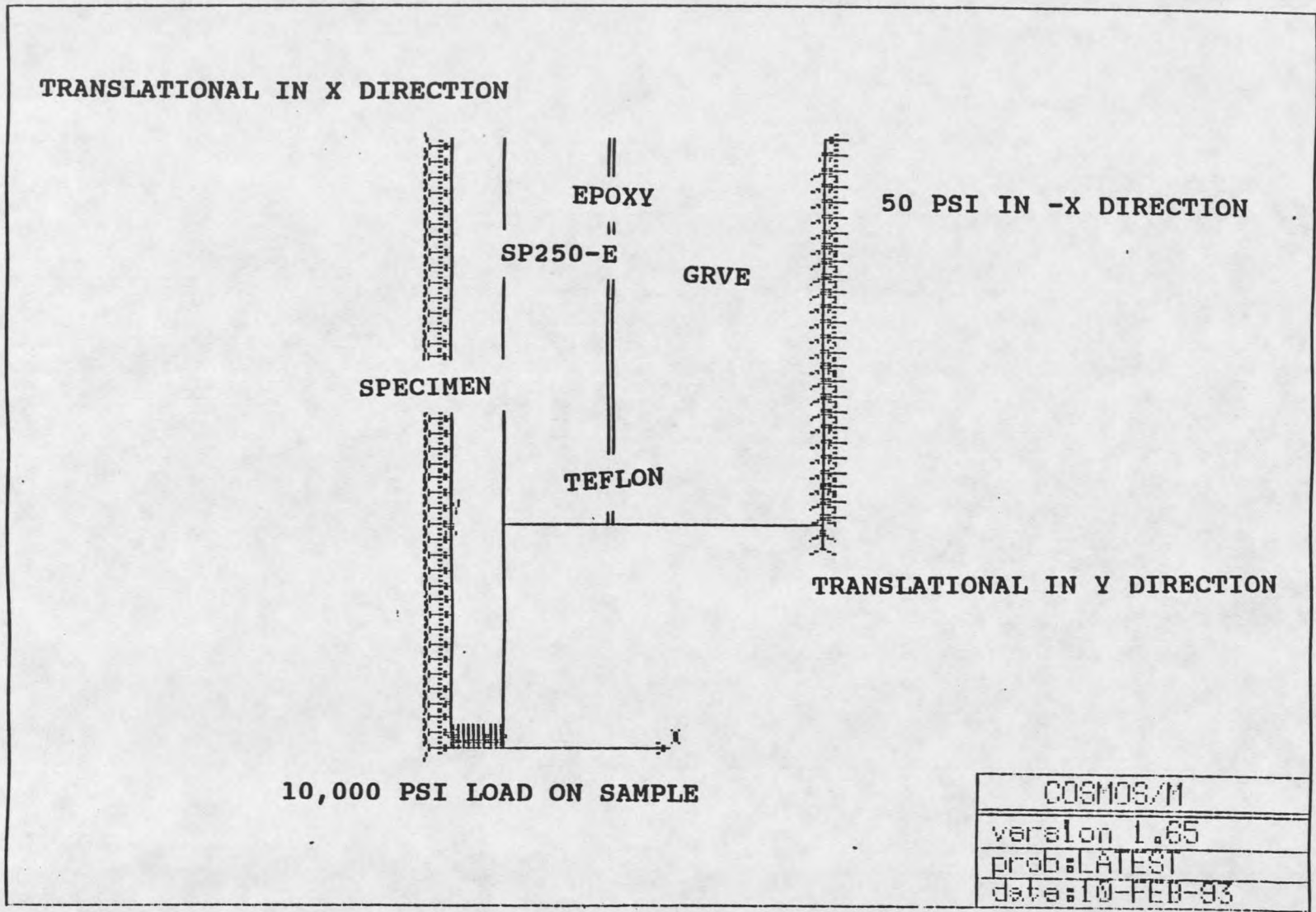
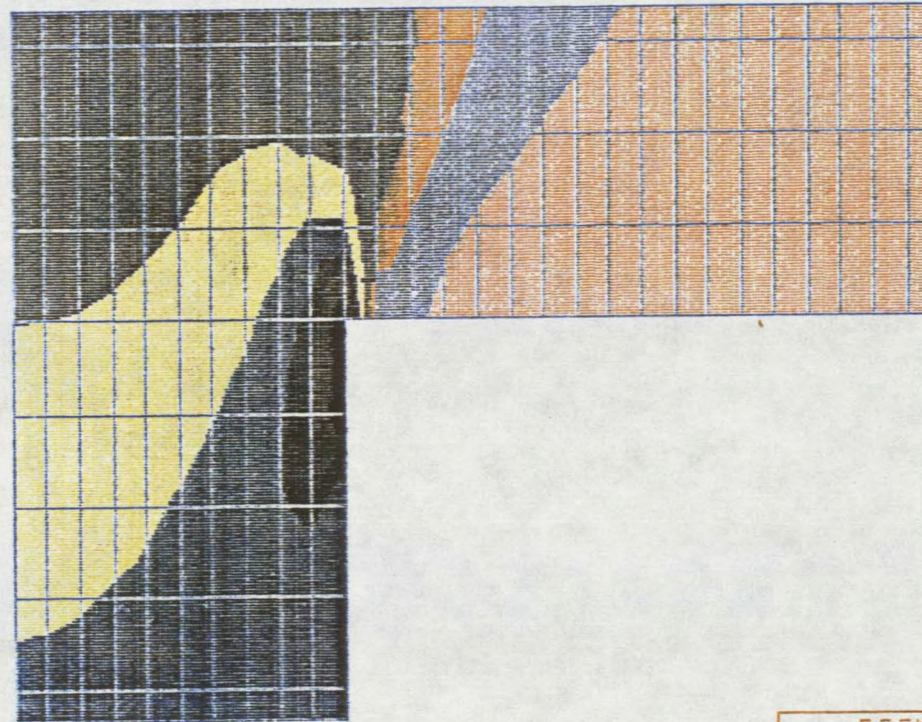


Figure 8. Boundary conditions for FEA of stress concentration with no epoxy layer next to the specimen.

L1n STRESS Lc=1



Sigma_Y	
1.84E+04	
1.45E+04	
1.27E+04	
1.08E+04	
8.91E+03	
7.04E+03	
5.17E+03	
3.29E+03	
1.42E+03	
-449.0000	



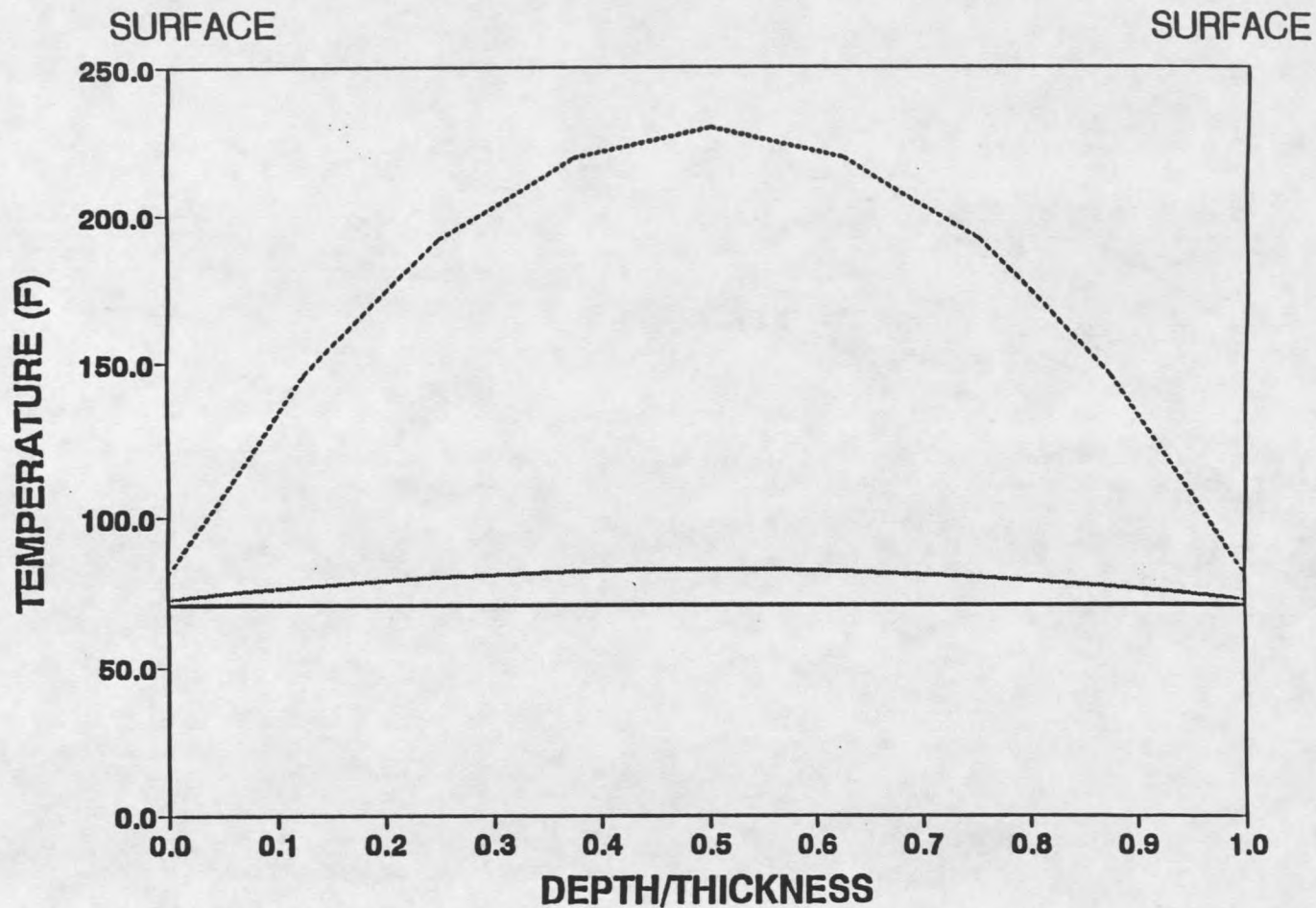
COSMOS/M
version 1.65
prob:LATEST
date:10-FEB-93

Figure 9. FEA results showing higher stress concentration with no epoxy layer next to the specimen.

that the thin layer of soft material makes a significant difference in the stress concentration. This would also probably be true if discrete fibers and matrix were modelled in the specimen.

The other finite element model was of the heat transfer in the specimen. The model is of a cross section in two dimensions, run for several thicknesses. Input variables were obtained as follows: the convection coefficient of air on the surface was obtained from Geankopolis [28], the heat transfer coefficient for polyester and vinylester matrix/fiberglass was obtained from Reference [24], and the heat generation term is an order of magnitude approximation from a damping test and a computer program hysteresis analysis (see Appendix B for these tests).

The model of the actual specimen at 100 Hz with the best approximations of the constants gave a temperature plot that was between the limits of 71.0° F in the center (mid-thickness), and 70.8° on the surface. On the progressively thicker specimens, the temperature at the center increases, which is observed experimentally [2]. Figure 10 shows the results for the three different trials with the depth into each specimen normalized by its thickness. For a specimen that is 16 times as thick as the test specimen, under the same conditions, the center of the specimen is over 225° F. The temperature where polyester begins to yellow is near 175° F (experimentally determined), which is an indication



SPECIMEN THICKNESS:

— 0.017 IN. THICK — 0.068 IN. THICK - - - 0.272 IN. THICK

Figure 10. FEA heat transfer results of temperature versus normalized distance for progressively thicker specimens.

of damage. The following table shows the results of the finite element models:

Table 2. Summary of Finite Element Analysis of Heat Transfer, 100 Hz.

Model Name	Heat1	Heat2	Heat3
Thickness	0.0017 in.	0.068 in.	0.272 in.
Center Temp.	71.0° F	83.0° F	229° F
Surface Temp.	70.8° F	73.3° F	84.5° F

In order to model the worst case scenario, the model was expanded to involve the tab region and the change in heat generation with differing stresses. Hysteresis based heat generation is assumed to vary with the square of the stress level for most materials, so the stress at different points could be related to the amount of heat generation at a particular point. The regions of stress (from the stress analysis) were then scaled for the amount of heat generation and the analysis was run (Figure 11). The essential finding is that even though the amount of stress in the tab region goes up slightly and the effective thickness goes up significantly, there appears to be little added heating of the specimen.

Experimentally, the surface temperature was monitored during testing at up to 100 Hz by using Omega Templog. The lowest temperature paint melts at 125° F, and was not observed melting on any specimen. This supports the results of the finite element analysis, and establishes the

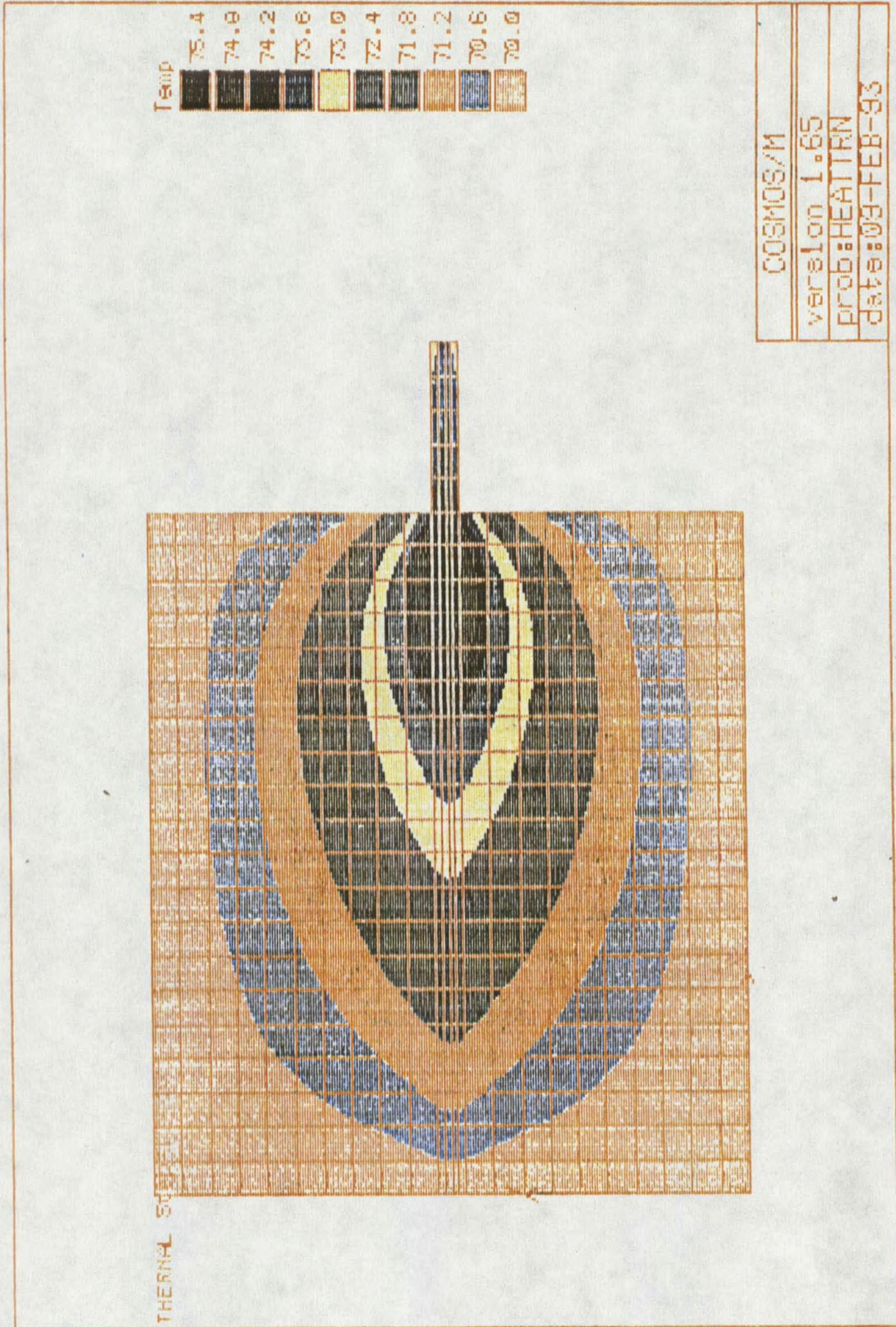


Figure 11. FEA heat transfer results showing heat dissipation into the tab region.

viability of the test method for high frequencies.

Stress Versus Number of Cycles Results

The maximum stress versus number of cycles to failure (S/N) data for the unidirectional E-glass/polyester composite are given in Figure 12. There are two trend lines for comparison. The linear equation, with a slope of ten percent of the one cycle strength per decade of cycles, has been shown to fit a variety of E-glass composites with well aligned fibers, as discussed above. The power law trend is a least squares fit to the data, forced through 1.0 at one cycle.

Representative specimens broken at different stress levels and frequencies can be seen in Figure 13. One characteristic of all failures was the development of axial splits in the specimens at different times depending on the load level. The high load level test specimens developed axial cracking on the first cycle, but the high cycle tests only showed these cracks after some period of cycling. For example, the first test run at the 20.5 percent load level did not have any axial cracking until over half the total number of cycles had been run. This damage began at a wave in the material (Figure 2), where most of this type of damage originates. Little other damage was evident prior to total failure, similar to observations with larger unidirectional coupons [2].

For comparison with literature S/N data, Figure 14 has

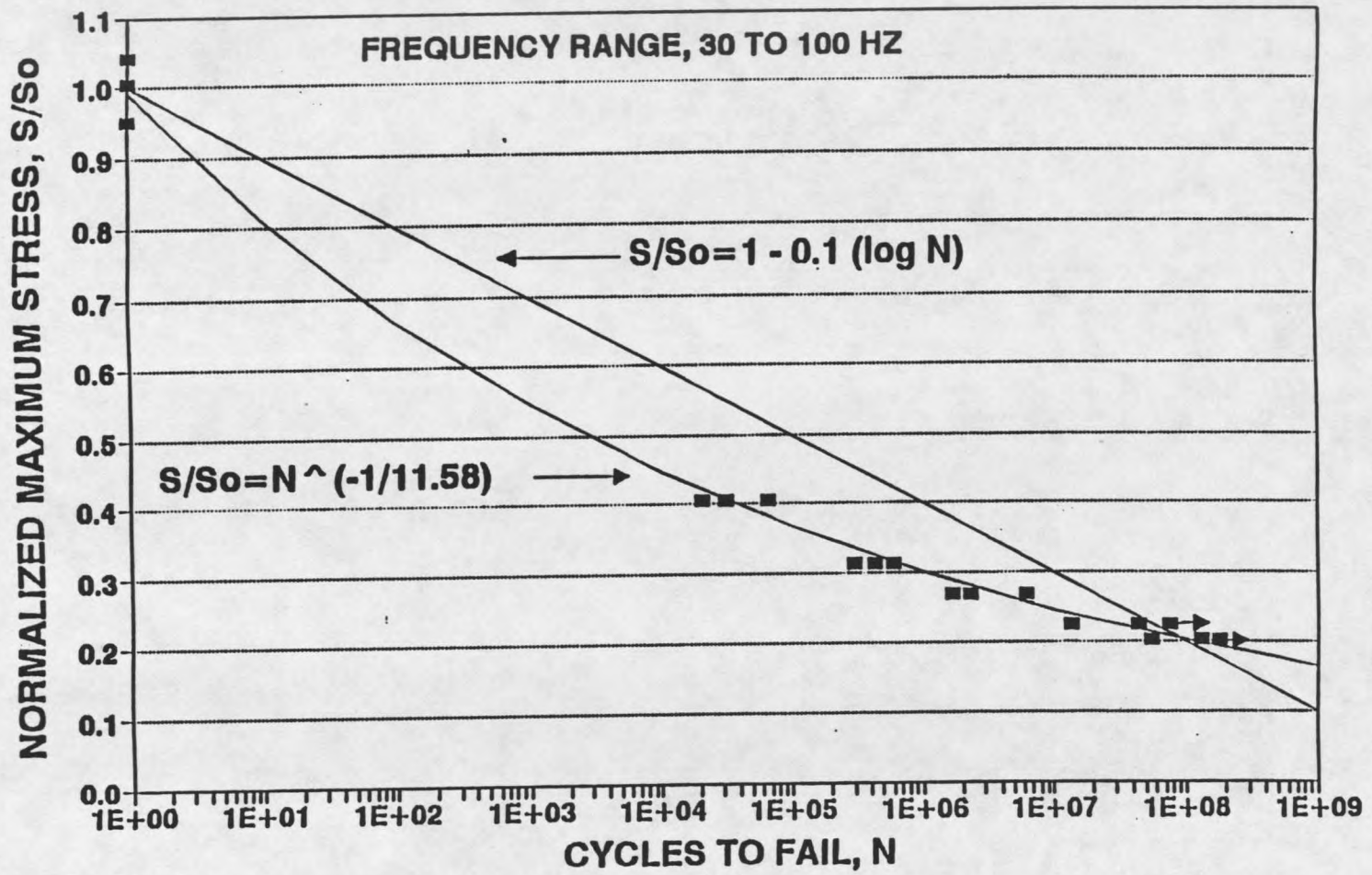


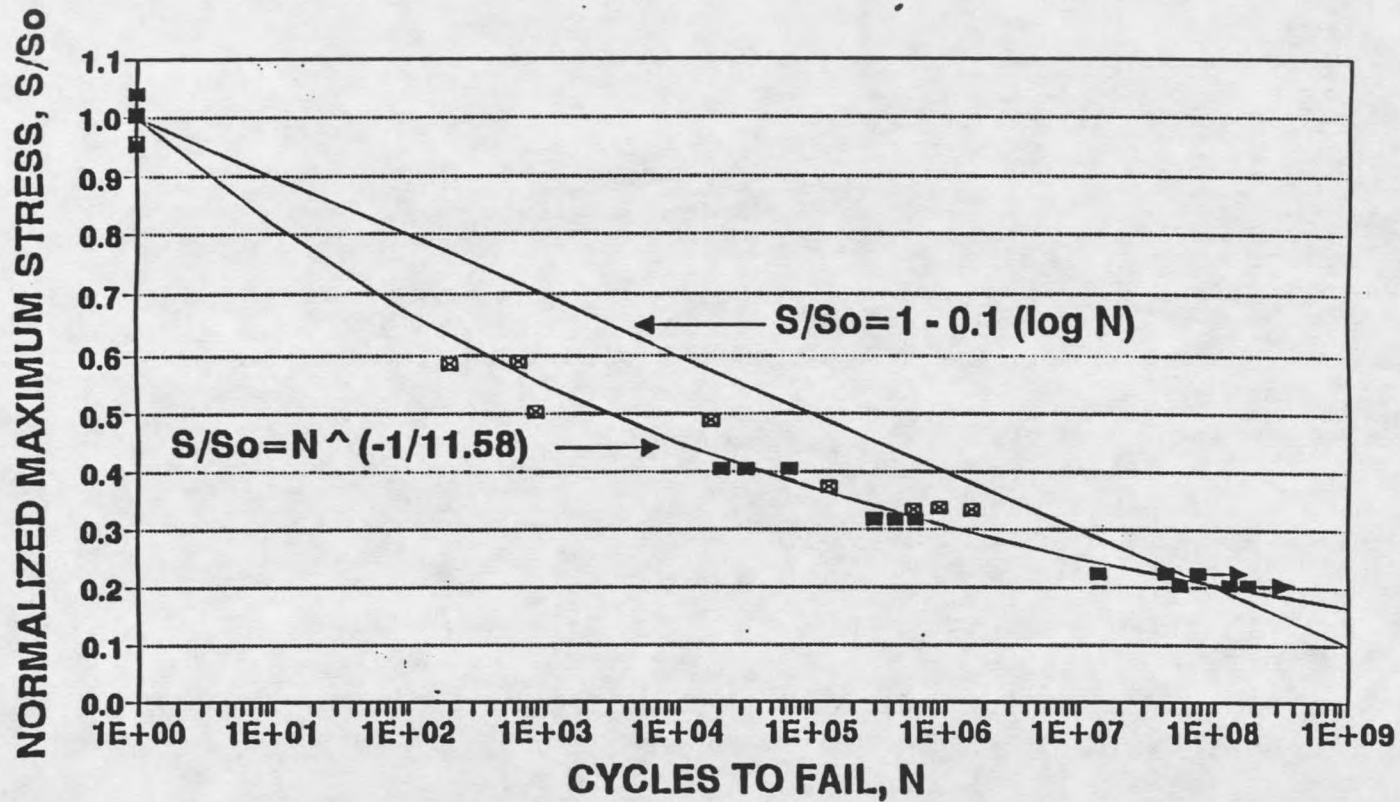
Figure 12. Normalized S/N curve of high frequency fatigue tests.



Figure 13. Photograph of typical broken specimens from different load levels and frequencies.

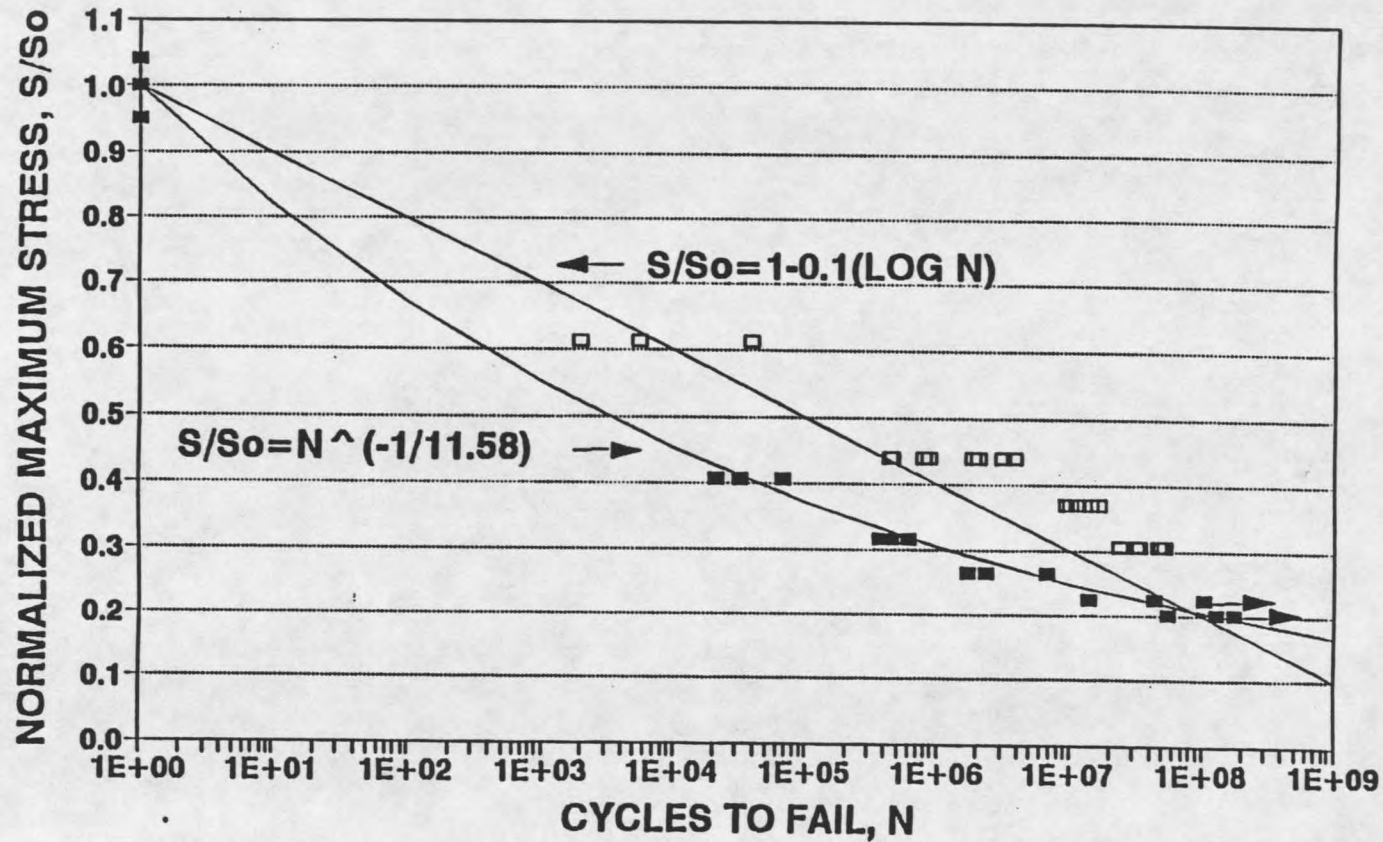
standard coupon data from a thesis by Reed [2] on the same plot as the data from this study. Both materials were unidirectional E-glass reinforced polyester, a standard coupon being in the form of 2 in. wide by 0.125 in. thick by 4 in. gauge section length tested at up to 10 Hz. Our tests were conducted at from 30 to 100 Hz. As can be seen, the data for both cases fall close to the same trend line, when both are normalized against their respective ultimate strengths. The ultimate strength for material A was 80,000 psi [2], while the ultimate strength for our case was 94,200 psi. This demonstrates that the specimen in question gives results in fatigue which agree with literature data in the moderate cycle range.

Also for comparison, Figure 15 shows an S/N curve with both our data and published data from Bach [8]. Specimen geometry used by Bach was unidirectional reinforced glass fiber/polyester plate (0.2 in. thick) machined into specimens with dimensions of 6.7 in. by 0.98 in. with a gauge section length of 3.1 in. The discrepancy between the two data sets may be attributable to the quality of the materials tested: typical windmill materials have a large amount of fiber misalignment which may be responsible for lower failure lifetimes, while prepreg or nonwoven specimens tend to have better alignment. Better alignment may result in less matrix splitting damage from stress concentrations caused by fibers even slightly off axis [19].



■ PRESENT STUDY (30-100 HZ) ☒ DATA FROM REED [25] (STD COUPON, 1-10 HZ)

Figure 14. Normalized S/N curve comparing high frequency data to windmill material standard coupon data.



\square DATA FROM BACH [6] \blacksquare PRESENT STUDY

Figure 15. Normalized S/N curve comparing high frequency data to well aligned standard coupon data.

Bach [8] speculated on the presence of a fatigue limit in the range of one billion cycles. While a fatigue limit in this range is possible, its presence could depend on any number of factors such as axiality of fibers, fiber/matrix bond strength, fiber/fiber interactions, etc. Since the trends for the two types of material are quite different at high stress levels, there could be a significant role of fabrication technique. However, trends for windmill blade materials and well aligned materials appear to be converging in the high cycle range. This could imply that layup technique has a decreasing impact on material properties in the low stress/high cycle range.

Our data has a calculated power law exponent of -11.58 when the fit is forced through 1.0 at one cycle. Others have reported this trend to be as high as -13.5 [2, 29], but the data used for that fit only went to moderate cycles. When our data are correlated in Figure 16 disregarding the high stress level tests (above $S/S_o=0.35$), the exponent of the power law rises to -13.7, consistent with the above reported trend. When our high cycle data are correlated using a semi-logarithmic fit, the slope of the trend line becomes -0.04, which is considerably lower than previously reported trends (Equation 1). These two curve fits include run-out data (specimens that do not break after long periods of testing, shown by arrows), which makes the steepness of the slopes conservatively high (Figure 16).

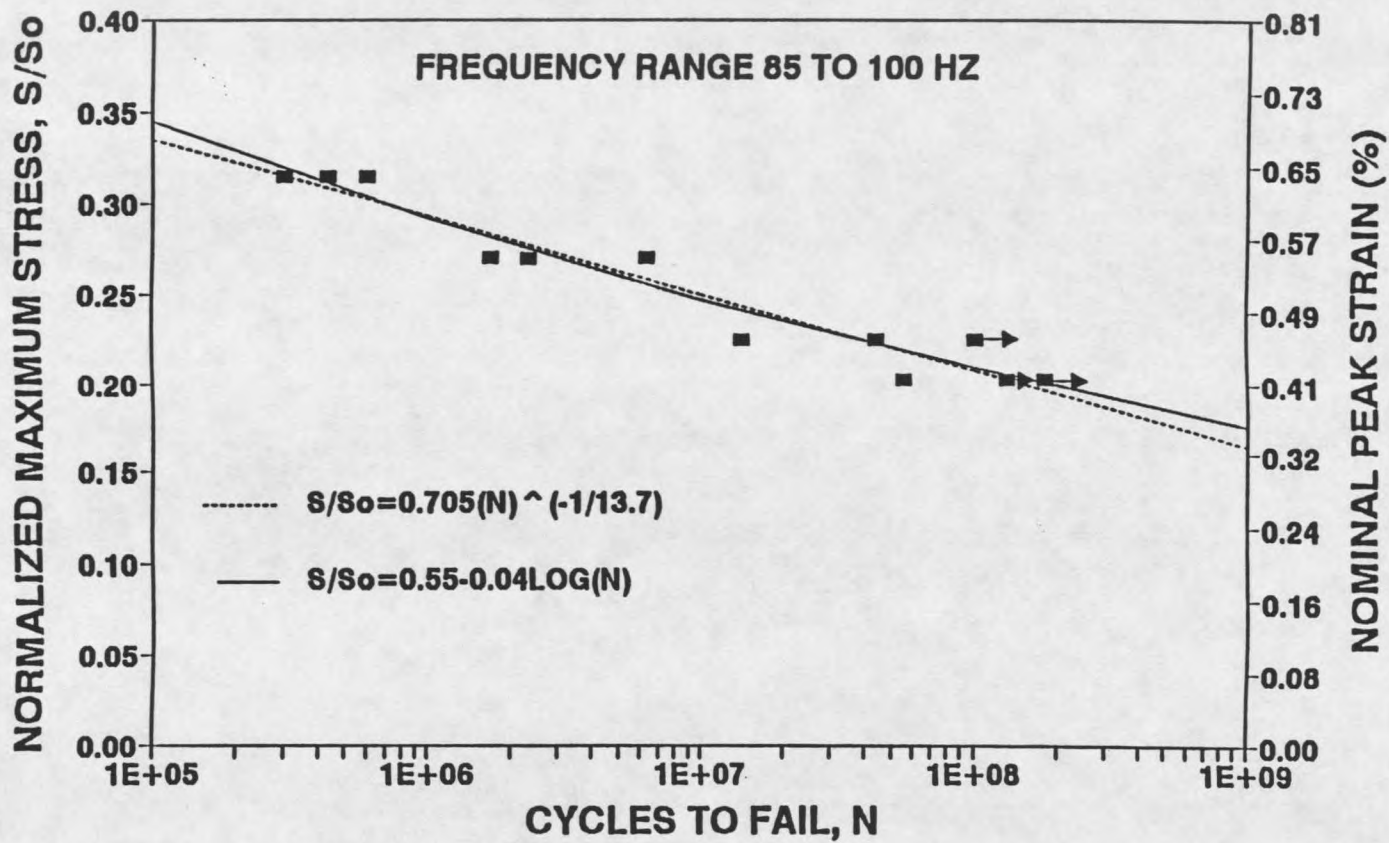


Figure 16. High cycle specimen data with points fit to power law and semi-logarithmic curves.

The correlation of fit (R) for the data are 0.932 for the semi-logarithmic fit and 0.972 for the power law fit. When either of these curve fits are extrapolated to 10^9 cycles, the design strain level is about 0.32 percent initial peak strain (peak stress/Young's Modulus). These strain levels are lower than reported in other studies [2,8]. The apparent reason for this is that the static strength (95,000 psi) is low for this fiber content and elastic modulus, giving a static failure strain ($E_t/95,000$ psi) of only 1.8 percent. Measured values appeared somewhat higher, but were still lower than the expected 2.5 to 3 percent. The apparent reason for the low strains is the waviness of the strands (Figure 2).

Complete data for this study are given in Table 3.

Table 3. Raw data.

% UTS	Cycles to Failure	Frequency (Hz)	Nominal Peak Strain (%)
95.0	1	4000 lb/sec	
100	1	4000 lb/sec	
104	1	4000 lb/sec	
40.5	67337	30	0.875
40.5	32127	30	0.875
40.5	21085	30	0.875
31.5	446549	75	0.601
31.5	432517	75	0.601
31.5	370661	75	0.601
31.5	382287	75	0.601
26.5	1685308	85	0.512
26.5	2323003	85	0.512
26.5	6727798	85	0.512
22.5	16254877	100	0.420
22.5	106706455*	100	0.420
22.5	43758798	100	0.420
20.2	55000000	100	0.397
20.2	130000000*	100	0.397
20.2	180000000*	100	0.397

* Run out tests, no failure

Frequency Effect

The data plotted in Figure 14 suggest no strong effect of frequency or size of specimen on the fatigue results. In order to more directly address the question of frequency effects, specimens were run at 10 and 70 Hz at the same load level, to see if the specimens tested at the two frequencies

would fail at the same number of cycles.

The following table shows the results of testing at a maximum stress (stress = load/cross sectional area) of 31.5 percent of the ultimate strength:

Table 4. Frequency Effect Data.

Cycles to Failure	Frequency (Hz)
446,549	75
432,517	75
370,661	75
382,287	75
1,695,536	10
910,256	10
512,659	10

Waveforms shown in Figures 17 and 18 are of typical load versus time traces obtained from a single specimen at the different frequencies. Waveforms shown in Figures 19 and 20 are of typical absolute displacement versus time from the same specimen as above. Both sets of plots show a similar sine wave pattern, precise to three significant figures. Thus, the load and displacement waveforms are similar at the two frequencies, but the 10 Hz specimens appear to last longer on average. It would be expected that the lower frequency tests would break with slightly fewer cycles [20], but this was not the case. This is a minor frequency effect, corresponding to an S/S_0 difference from 0.41 down to 0.37 using the median values. The origin of the effect requires further study.

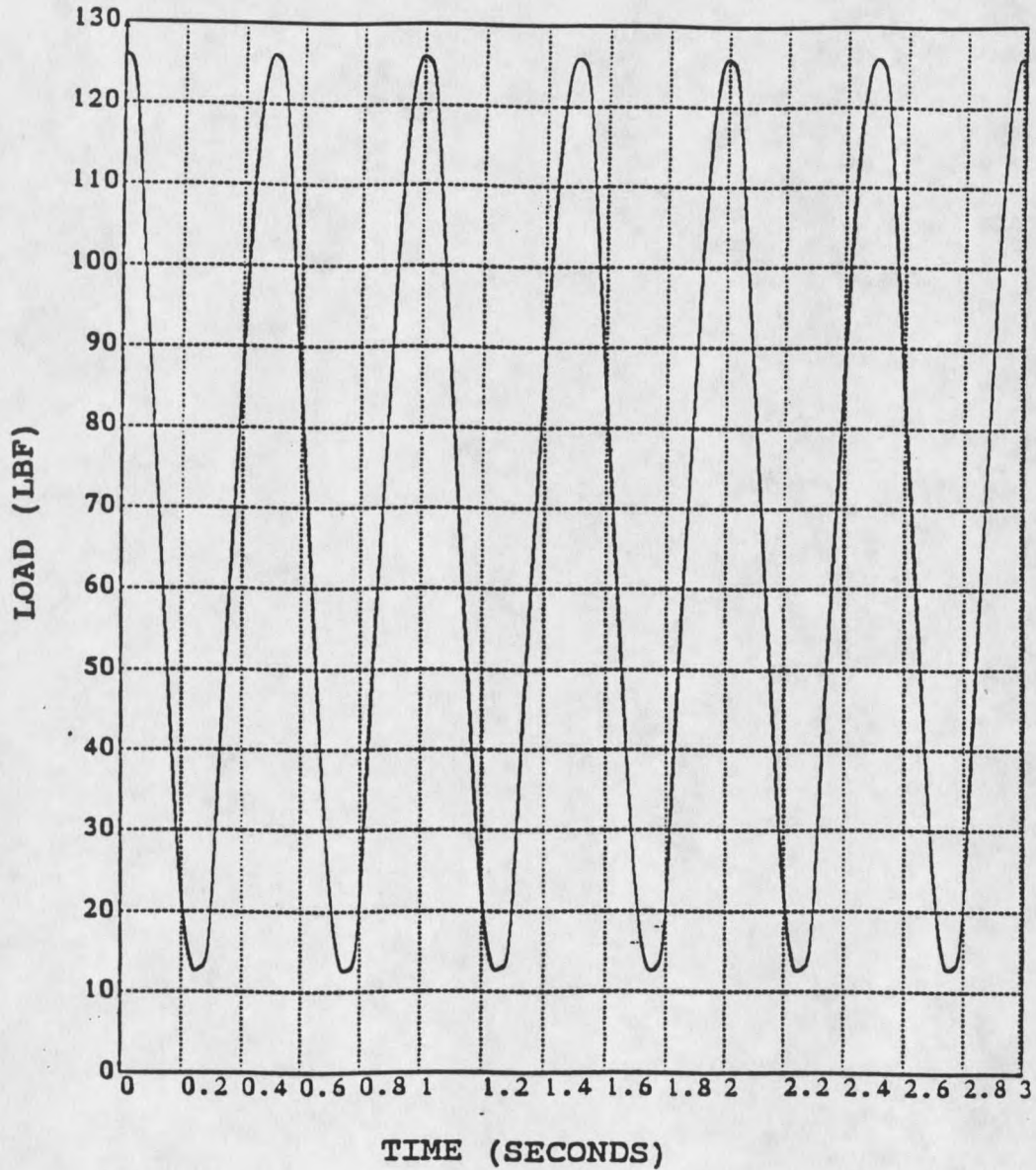


Figure 17. Load versus time plot for specimen running at 10 hertz.

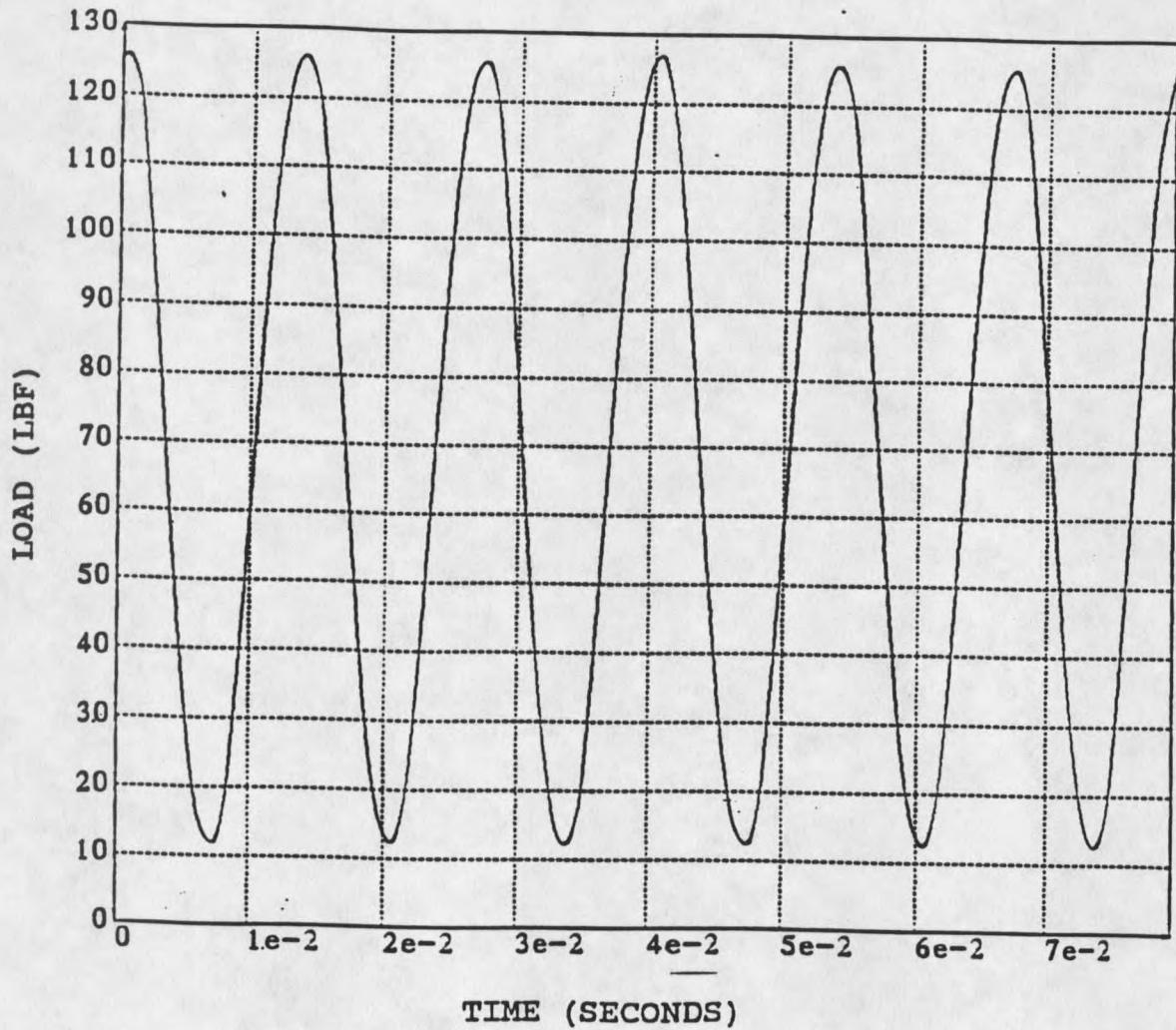


Figure 18. Load versus time plot for specimen running at 75 hz.

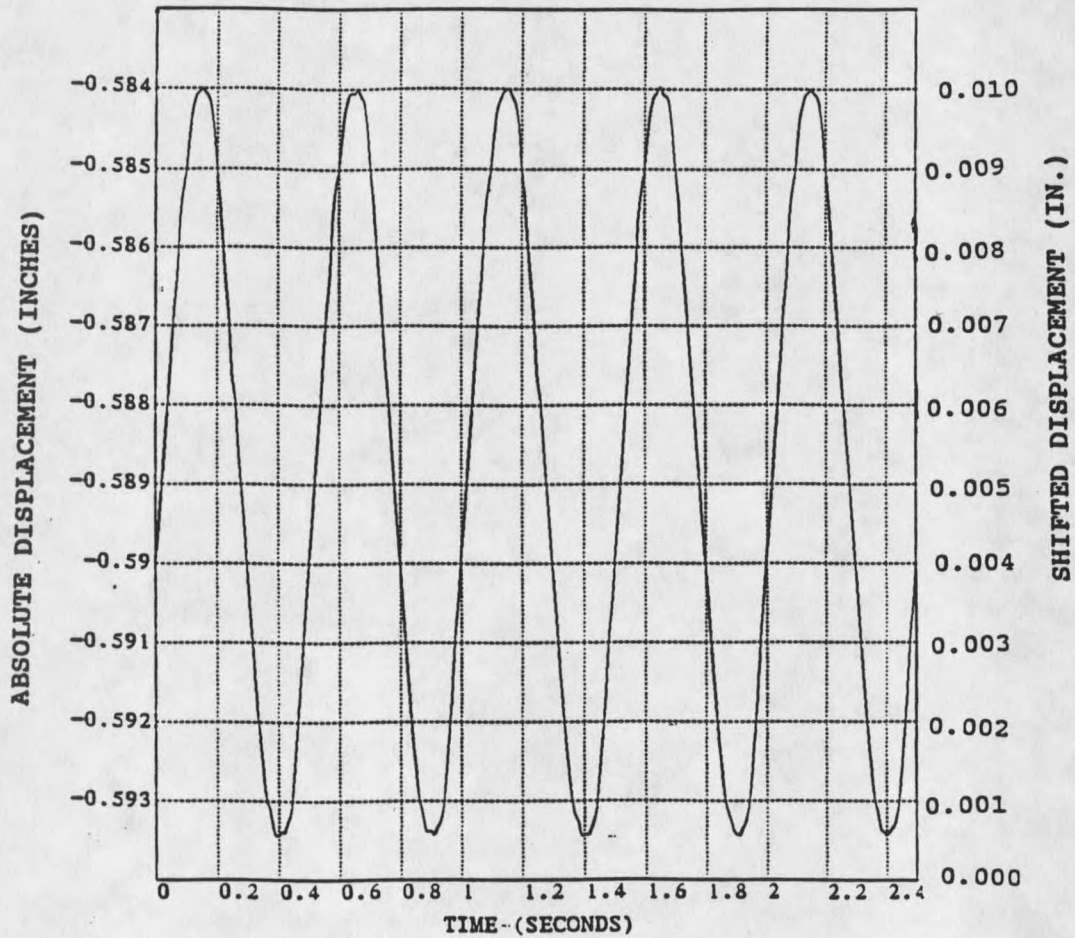


Figure 19, Displacement versus time plot for sample running at 10 hz.

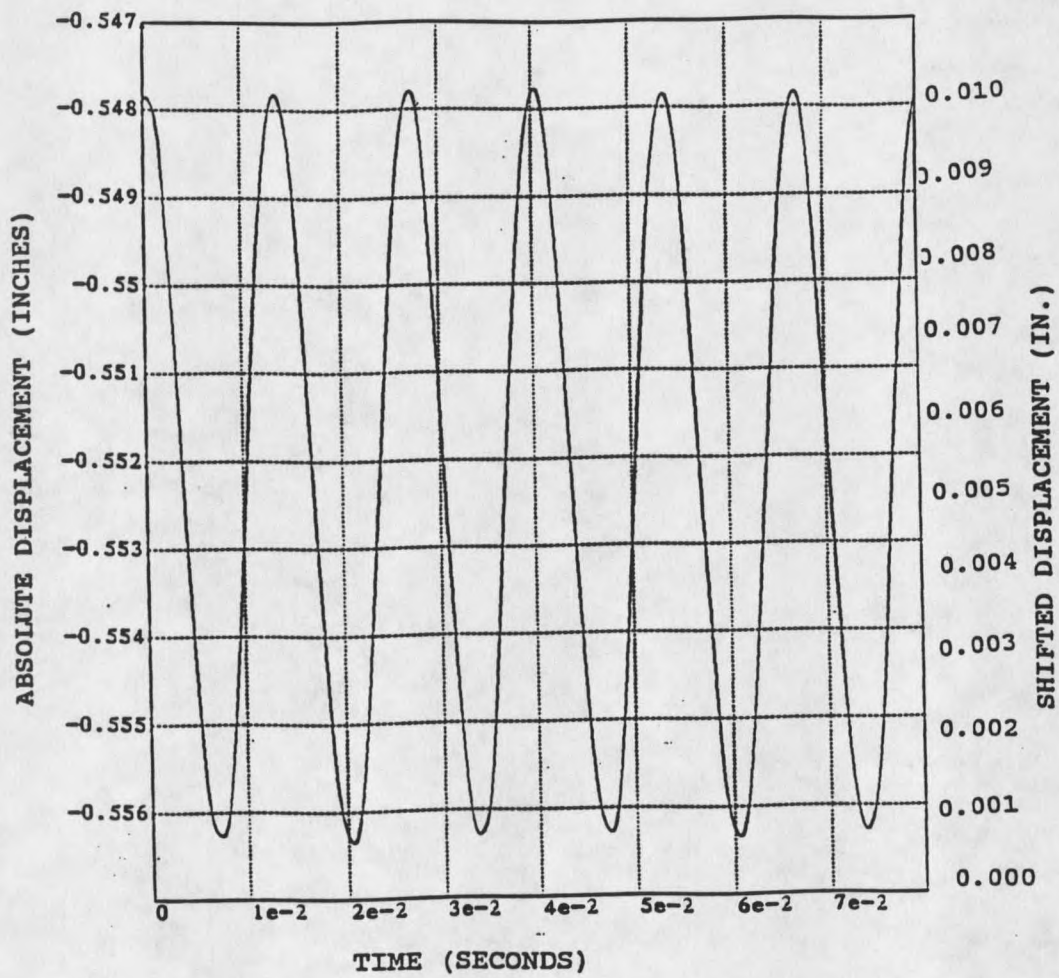


Figure 20. Displacement versus time plot for specimen running at 75 hz.

CHAPTER FIVE**CONCLUSIONS AND RECOMMENDATIONS**Conclusions

The purpose of this study was to develop a test method suitable for obtaining high cycle fatigue data in a reasonable amount of time. Test results are given for unidirectional E-glass reinforced polyester similar to that used in wind turbine blades. Data on material lifetime were obtained at several stress levels at cycles to 180 million and frequencies to 100 Hz. These are the first known published data in this region for composite materials. Conclusions are based on tests run in load control with sinusoidal loading at $R = 0.1$.

Since the primary purpose of the study was to develop a test method, some qualification of the specimen geometry was necessary. Finite element analyses of the specimen were carried out. These showed that the specimen would not heat significantly at 100 Hz, and that the stress concentration at the tabs was low. These results were supported experimentally by surface temperature measurements and careful examination of specimens during testing and after fracture.

The S/N data obtained out to the range of windmill

fatigue lifetimes show that fiberglass has a less steep S/N trend at lower stress levels. At higher stress levels, lifetime is dependent on axial matrix/interfacial cracks, due at least in part to fiber misalignment, and failure may be more matrix dominated. At lower stresses, the fatigue limit of the matrix may be reached and some type of overall composite fatigue limit approached. This conclusion is based on the fact that the higher stress tests showed axial splitting after some amount of cycling; the splits increased in number as further cycling was done. With the lower stress tests, there were no axial splits prior to failure. Since the S/N curve for polyester has a very low slope [30], and appears to level off at under 100 thousand cycles, the exhaustion of the matrix splitting could be a direct result of reaching the fatigue strain limit or crack growth threshold of the matrix.

Differences in fatigue curves between Bach and those by Reed and the author could partially be attributed to the materials used. Materials used by Bach showed a significantly higher resistance to fatigue at high stress levels, however, at low stresses the two trends were converging. This would lead to the conclusion that in the stress and cycle range of interest, factors other than the quality and size of specimens may dominate fatigue behavior.

The test method developed in this study should be adaptable to other failure modes and types of loading. More

complete stress amplitude and mean stress conditions can now be studied to develop Goodman-type plots at 10^8 cycles. While little effect of specimen volume is noted in comparison with standard coupons about 100 times larger (Figure 14), there does appear to be a sensitivity to imperfections such as fiber misalignment (waviness, Fig. 2).

Recommendations

Results of this research established the basic strength reduction patterns for above one million cycles due to fatigue loading at $R = 0.1$. With present equipment it is possible to run spectrum loading on a specimen; this type of loading would give a better representation of the behavior of the material in the cycle range of interest. Since this technique makes long term tests possible in a short amount of time, and the WISPER [31] program is available, testing should continue with spectrum loading, allowing for the changing of design criteria for blades in as short of time as possible. The material tested represents the material in a blade, and with this comes some fiber misalignment, porosity, and some potential misalignment with the load direction. To determine fundamental material properties, use of single layer of prepreg for specimens, aligned exactly with the load train would probably give less scatter and higher static properties. Comparisons with data by Bach showed that premium materials make a considerable difference

in the high stress fatigue life of composites. Also, the strain levels to produce failure at high cycles are notably higher in Bach's case.

From the heat transfer data, it appears that heating of the specimen may not be a problem for up to four layers of material, so thicker specimens may be tested. Since the loss factor, and therefore the heat generation, seems to be much more dependent on the amplitude of the stress and not the peak stress, thicker specimens could potentially be used on the long term high cycle tests.

One of the fundamental problems with present windmill materials is the way the reinforcement is made. With even these small volume tests, the material has waviness and is not aligned well. With reinforcement fabric, there are not only problems with the reinforcement itself, but in most cases it is stitched together with organic thread, giving rise to further stress concentration problems. One thing that may help immediately with material properties is to use a bonding agent instead of stitching, and somehow keep the waviness in the unidirectional rovings to a minimum.

The most important factor in initial damage development with small volume testing appears to be matrix cracking at waves in the material. If the power law holds true for more axial fiber alignment without this waviness, the peak strain values for design may improve, allowing for design of lower weight turbine blades.

REFERENCES

REFERENCES

1. "Assessment of Research Needs for Wind Turbine Rotor Technology", Report of the Committee on Assessment of Research Needs for Wind Turbine Rotor Materials Technology, National Research Council, National Academy Press, Washington D.C., 1991.
2. Reed, R. M. "Long Term Fatigue of Glass Fiber Reinforced Composite Materials for Wind Turbine Blades", Montana State University Masters Thesis, 1991.
3. Reifsnider, K. L., "Damage and Damage Mechanics" in Fatigue of Composite Materials, Reifsnider, K. L. ed., Elsevier Science Publishers, New York, pp. 11-75, 1990.
4. Owen, M. J., and Dukes, R., "Failure of Glass-Reinforced Plastics Under Single and Repeated Loading", Journal of Strain Analysis, vol. 2, no. 4, pp. 272-279, 1967.
5. Dharan, C. K. L., "Fatigue Failure Mechanisms in a Unidirectional Composite Material" in Fatigue of Composite Materials, STP 569, American Society for Testing Materials, Philadelphia, pp. 171-188, 1975.
6. Owen, M. J., "Fatigue Damage in Glass Reinforced Plastics" in Fracture and Fatigue, Broutman, L. J. ed., Academic Press, New York, pp. 337-339, 1974.
7. Boller, K. "Composite Materials Testing and Design", ASTM STP 460, American Society for Testing Materials, p. 217, 1969.
8. Bach, P. W., "High Cycle Fatigue Testing of Glass Fibre Reinforced Polyester and Welded Structural Details", Netherlands Energy Research Foundation ECN, The Netherlands, 1991.
9. Salkind, M. J., "Fatigue of Composites", Composite Materials: Testing and Design (Second Conference), ASTM STP 497, American Society for Testing Materials, pp. 143-169, 1972.

REFERENCES- Continued

10. Broutman, L. J. and Sahu, S. "Progressive Damage of a Glass Reinforced Plastic During Fatigue", Proceedings of the Reinforced Plastics and Composites Institute Annual Conference, vol. 11, section 11-D, New York, pp. 1-12, 1969.
11. Rotem, A. "Fatigue and Residual Strength of Composite Laminates", Engineering Fracture Mechanics, vol. 25 nos 5/6, pp. 819-827, 1986.
12. Stinchcomb, W. W. and Bakis, C. E. "Fatigue Behavior of Composite Laminates" in Fatigue of Composite Materials, Reifsnider, K. L. ed., Elsevier Science Publishers, New York, pp. 107-108, 1990.
13. Mandell, J. F. et al, "Tensile Fatigue Performance of Glass Fiber Dominated Composites", Composites Technology Review, vol. 3, no. 3, pp. 96-102, Fall 1981.
14. Mandell, J. F. "Fatigue Behaviour of Fibre-Resin Composites" in Developments in Reinforced Plastics-2, Properties of Laminates, Pritchard, G. ed., Applied Science Publishers, London, pp. 67-107, 1982.
15. Shih, G. C. and Ebert, L. J. "The Effect of the Fiber/Matrix Interface on the Flexural Fatigue Performance of Unidirectional Fiberglass Composites", Composites Science and Technology, vol. 28, pp. 137-161, 1987.
16. Kensche, C. W., and Kalkuhl, T. "Fatigue Testing of GL-EP in Wind Turbine Rotor Blades", European Community Wind Energy Conference Proceedings, 1990.
17. Kensche, C. W. "High Cycle Fatigue of Glass Fibre Reinforced Epoxy Materials for Wind Turbines", DLR-Forschungsbericht 92-17, 1992.
18. Kensche, C. W., and Seifert, H. "Wind Turbine Rotor Blades Under Fatigue Loads", German Aerospace Research Establishment, Stuttgart, 1990.
19. Mandell, J. F., et al, "Fatigue Performance of Wind Turbine Blade Composite Materials", SED-vol. 14 ASME Wind Energy Conference, 1993.

REFERENCES-Continued

20. Mandell, J. F. "Fatigue Behavior of Short Fiber Composite Materials" in Fatigue of Composite Materials, Reifsnider, K. L. ed., Elsevier Science Publishers, New York, pp. 232-333, 1991.
21. McCrum, N. G., Buckley, C. P., and Bucknall, C. B., Principles of Polymer Engineering, Oxford University Press, New York, 1988.
22. Gibson, R. F., Yau, A., and Rienger, D. A., "Vibration Characteristics of Automotive Composite Materials" in Short Fiber Reinforced Composite Materials, ASTM STP 772, Sanders, B. A. ed., American Society for Testing Materials, pp. 133-150, 1982.
23. Mandell, J. F., and Meier, U., "Effects of Stress Ratio, Frequency, and Loading Time on the Tensile Fatigue of Glass-Reinforced Epoxy" in Long-Term Behavior of Composites, ASTM STP 813, O'Brian, T. K. ed., American Society for Testing Materials, pp. 55-77, 1983.
24. Engineered Materials Handbook Volume 1 "Composites" ASM International, 1988.
25. Modern Plastics Handbook, vol. 68, no. 11, McGraw Hill, New York, 1992.
26. 3M Material Data Sheet for Scotch Ply SP250E, 1992.
27. Engineered Materials Handbook, Volume 2 "Engineered Plastics" ASM International, 1988.
28. Geankopolis, C. J. Transport Processes and Unit Operations, Allyn and Bacon, Inc., Boston, 1983.
29. Mandell, J. F., Reed, R. M., and Samborsky, D. D. "Fatigue of Fiberglass Wind Turbine Blade Materials" SAND92-7005, Sandia National Laboratories, 1992.
30. Huang, D. "Tensile Fatigue of Short Fiber Reinforced Composites", MIT Doctoral Thesis, 1981.
31. Ten Have, A. A. V., "WISPER: A Standardized Fatigue Load Sequence for HAWT-Blades", Proceedings of the European Wind Energy Conference, Palz, W. ed., Stephens and Assoc., Bedford England, 1988.
32. Sendeckyj, G., Personal Communication, Wright Patterson Air Force Base, 1991.

REFERENCES-Continued

33. Gibson, R. F. "Damping Characteristics of Composite Materials and Structures" in Structural Composites, Design and Processing Technologies, ASM International, Materials Park, Ohio, pp.441-449, 1990.

APPENDICES

APPENDIX A
Specimen Development

Several different specimens and tabbing regimes were tried before the final one was arrived at. The original specimen had a single tab glued to one side of a specimen. This did not appear to work because the epoxy always broke before the specimen did. The ultimate load achieved from this trial was 220 lbf. From this came a two piece tab made of aluminum. These were shaped similarly to the "dogbone" shape of regular metal specimens. A groove was cut in the center for alignment and to insure a parallel surface for gripping. This again was unsuccessful because the specimen tended to break where the aluminum and the specimen came together. This did, however, improve the ultimate load level to 360 lbf.

It was thought that smaller specimens would reduce the stress concentration at the edge, so rovings about ten percent of the size of the initial stock were tried. This was discontinued because the specimens were being tested on an Instron model 8501 machine, with 22,480 pound capacity, and the sensitivity of the load cell was not high enough to test the specimens in fatigue. In most cases there was enough compressive stress to crush the specimen while the machine was going to zero load.

Larger specimens were then tried again with a different approach. A tab made of steel with a wedge taken out was the next trial. Specimens were cut to 2.5 inches and then

epoxy was molded on the ends in the same shape as the steel tab wedge. After curing, the specimens were slipped into the tabs and tested. The ultimate strength of this type of tab was again 360 lbf.

Finite element analysis of this type of tabbing showed the stress concentration to be quite high, and the epoxy tended to crack after very few fatigue cycles. Combatting the problem of cracking, random E-glass polyester mat was machined to the appropriate size and bonded on the specimen surface. The specimen was then, as before, put in the steel tabs. Figure 21 shows the random mat and steel tabbing case. This again did not work because of stress concentration on the specimen. In all the specimens using the steel tabbing, very soon into all the fatigue tests the specimens tended to crack parallel to the fibers, the cracks emanating from the tab region. This was further evidence of stress concentration problems.

All of the tab styles were tested in fatigue, where stress concentration problems arose. In single pull tests, the strength attained did not change much, but in fatigue problems were evident because of very large scatter. Some scatter is expected, but several orders of magnitude was unacceptable.

The final specimen was arrived at after some consideration of previous specimens. Problems generally emanated from a stress concentration at the tab, and,

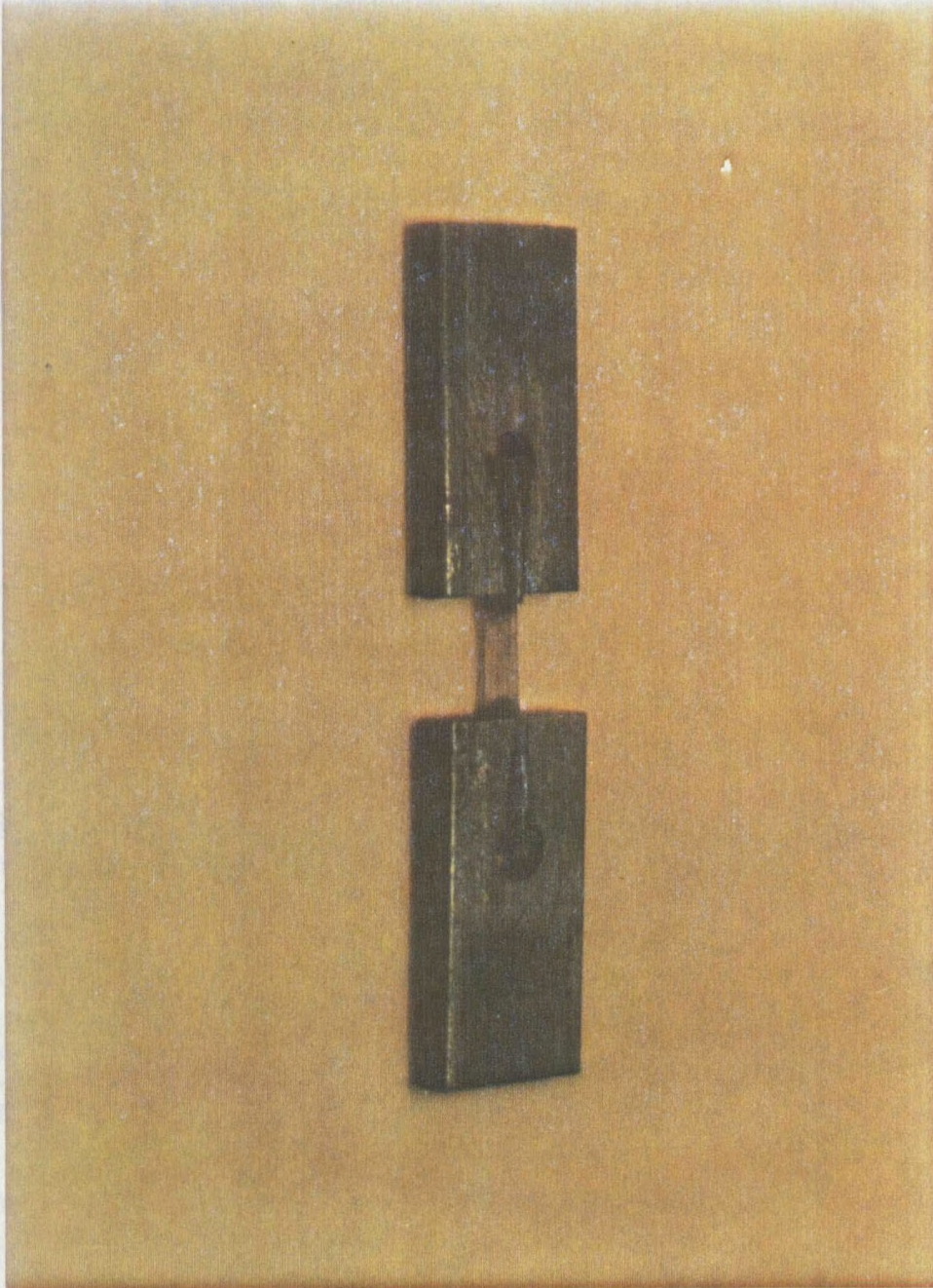


Figure 21. Initial tab for specimen.

therefore, this had to be eliminated. A trial of similar tabbing to standard coupon tabs was tried without much luck because the thin section always peeled away from the surface, causing damage to the specimen in the process. The final specimen follows a similar idea to the tapered tab, with the Teflon acting as the tapered region, as suggested by Sendekyj [32]. The material above the Teflon allows the specimen to be gripped all the way to the end, thereby eliminating the peeling problem, but makes the stress concentration in the direction of the load very small. However, the finite element analysis indicates that the Teflon does not contribute significantly, since it is positioned outside the first (unidirectional) tab layer.

APPENDIX B

Hysteresis

Two tests were performed to determine the value of the heat generation in fatigue. The general method for obtaining a loss factor is from Gibson [32]. A loss factor is defined as the ratio of the spread of the hysteresis curve divided by the maximum stress (Figure 22).

The subject material in this study was used for the first test, with a piece five inches long. The piece was bonded between two plates of 0.25 in. thick steel, with three inches protruding. A strain gauge was carefully aligned with the fibers and placed 0.25 in. from the steel. A ring stand was used with a rod mounted to hold the specimen at a particular strain level, for release with little friction in order that the specimen would oscillate up and down. A computer took data points at the rate of 500 per second and plotted the data as time versus strain level. Several tests were run on our material, but the results appeared to give values for the loss factor that were very high. For comparison, a more substantial specimen of unidirectionally reinforced polyester, 0.1 in. thick and 15 in. long was prepared in a similar fashion and tested. The loss factor for the larger piece was about one third the value for the first material. Figure 23 gives a representative response curve for the larger specimen. Since our material specimen was very thin, there was probably a significant amount of damping due to air friction and other effects which gives erroneous loss factors. Table

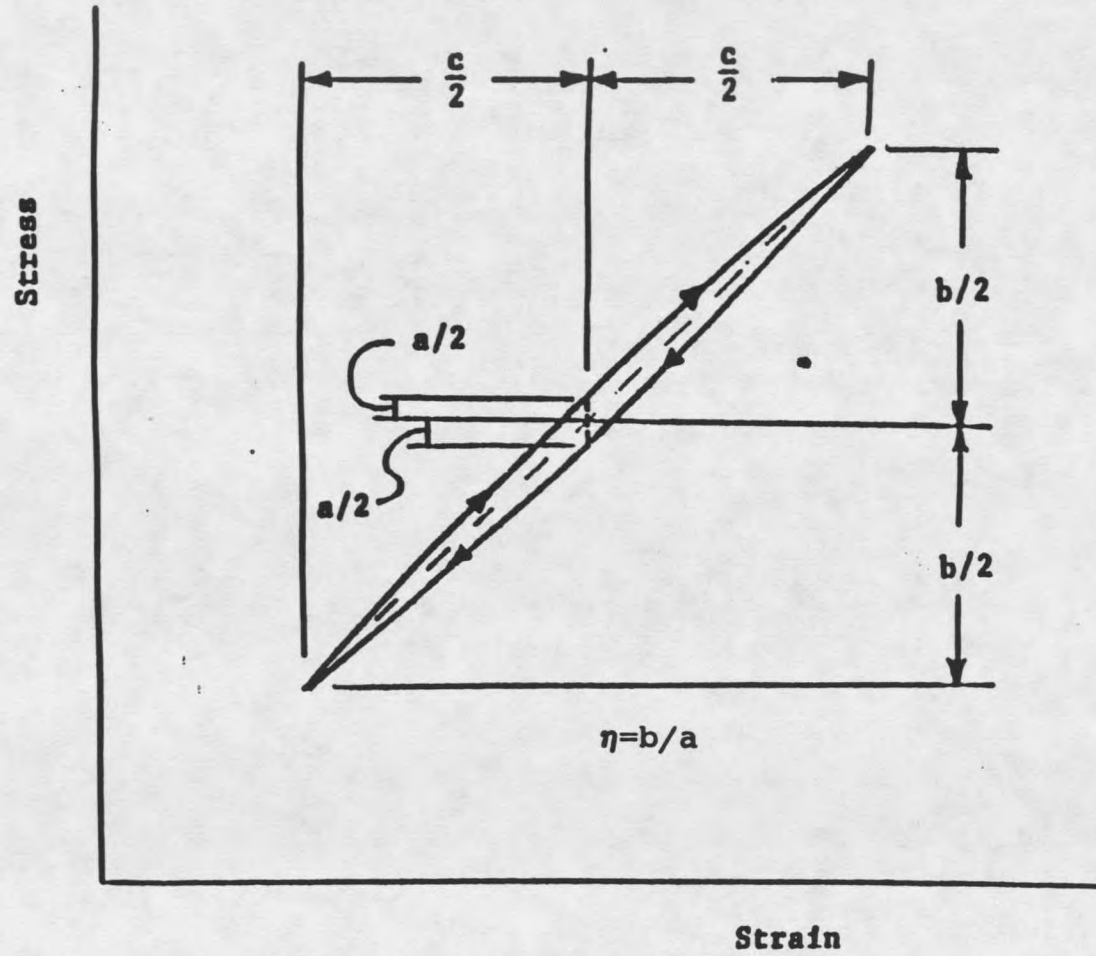


Figure 22. Hysteresis and the loss factor [30].

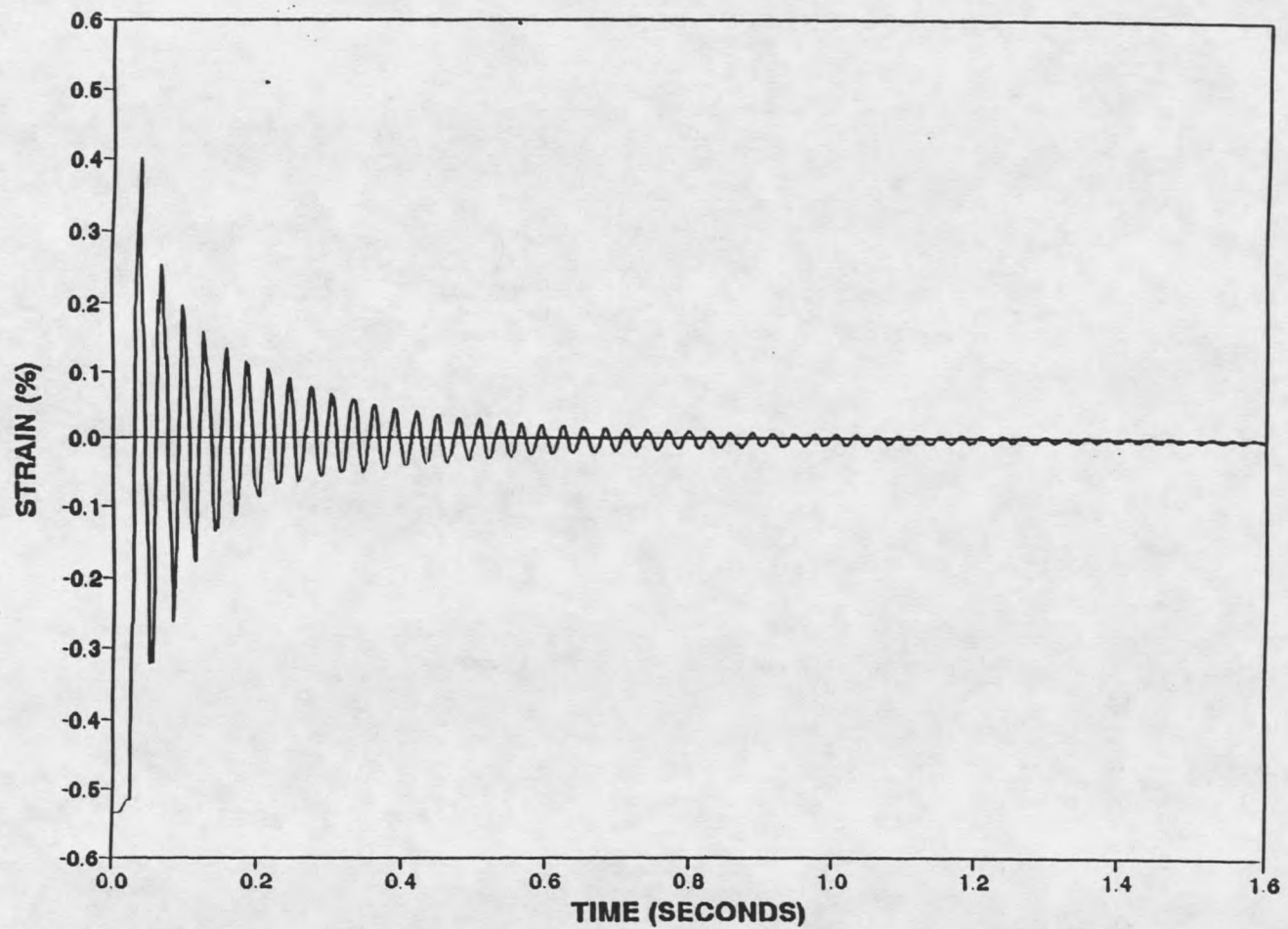


Figure 23. Time versus strain curve for unidirectional GRP.

5 shows the peak strain values and the associated loss factors (η) for the longer larger specimen.

Table 5. Loss Factors for Unidirectional Fiberglass Composite.

Peak Number	Strain (%)	η	Peak Number	Strain (%)	η
A1	0.486	0.033	C1	0.486	0.033
A2	0.439	0.033	C2	0.439	0.033
A3	0.396	0.034	C3	0.396	0.034
A4	0.356	0.036	C4	0.356	0.039
A5	0.317	0.017	C5	0.315	0.008
B1	0.539	0.027	D1	0.545	0.034
B2	0.495	0.032	D2	0.489	0.032
B3	0.447	0.034	D3	0.442	0.027
B4	0.402	0.036	D4	0.406	0.033
B5	0.359	0.031	D5	0.365	0.036

The loss factor average for the strain range in question is 0.033, and this was the value used in calculations. This loss factor was used for an order of magnitude approach to the amount of hysteresis in the specimen compared to the overall amount of energy for a single cycle.

A second approach was utilized to ensure the correct order of magnitude, and simply involved using Instron Flaps Five software to calculate hysteresis energy in the tensile fatigue tests. After running a test in computer control and taking as many as fifty data points per cycle, the software calculated a hysteresis value per cycle. This value came out to be approximately 0.01 in*lb/cycle. Converting this

to a constant heat generation for a specimen being tested at 100 hertz gives a value of 1×10^{-4} BTU/in sec. This is one order of magnitude higher than the value used in the finite element models. However, all model were rerun with this value and resulting temperatures were not significantly different. For example, the model of the actual specimen had a center temperature of 71.0° F, and with the higher heat generation value the center temperature was 73.4° F.

APPENDIX C

Grips for the Instron 8511

Grips for the Instron 8511 were fabricated during this study. The basic pattern was derived from existing grips. To improve the grip, a thin piece of 240 grit emery cloth was added on each side of the grip faces to add to the friction between the grip and the specimen. The round shape was used to limit the weight as compared to rectangular stock. Figure 24 is a schematic of the grips, and Figure 25 is a photograph of them with a specimen running.

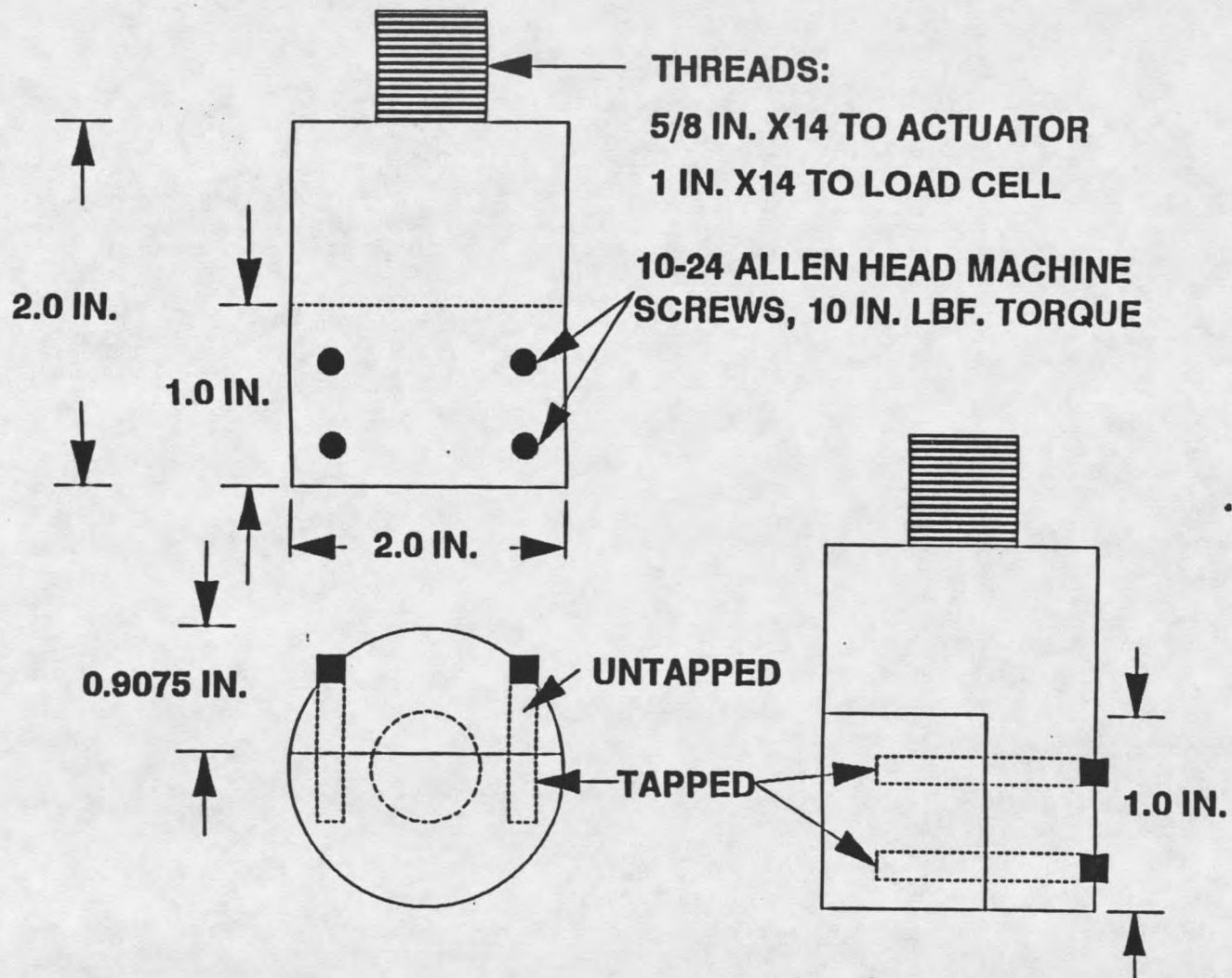


Figure 24. Schematic of Instron 8511 grips.

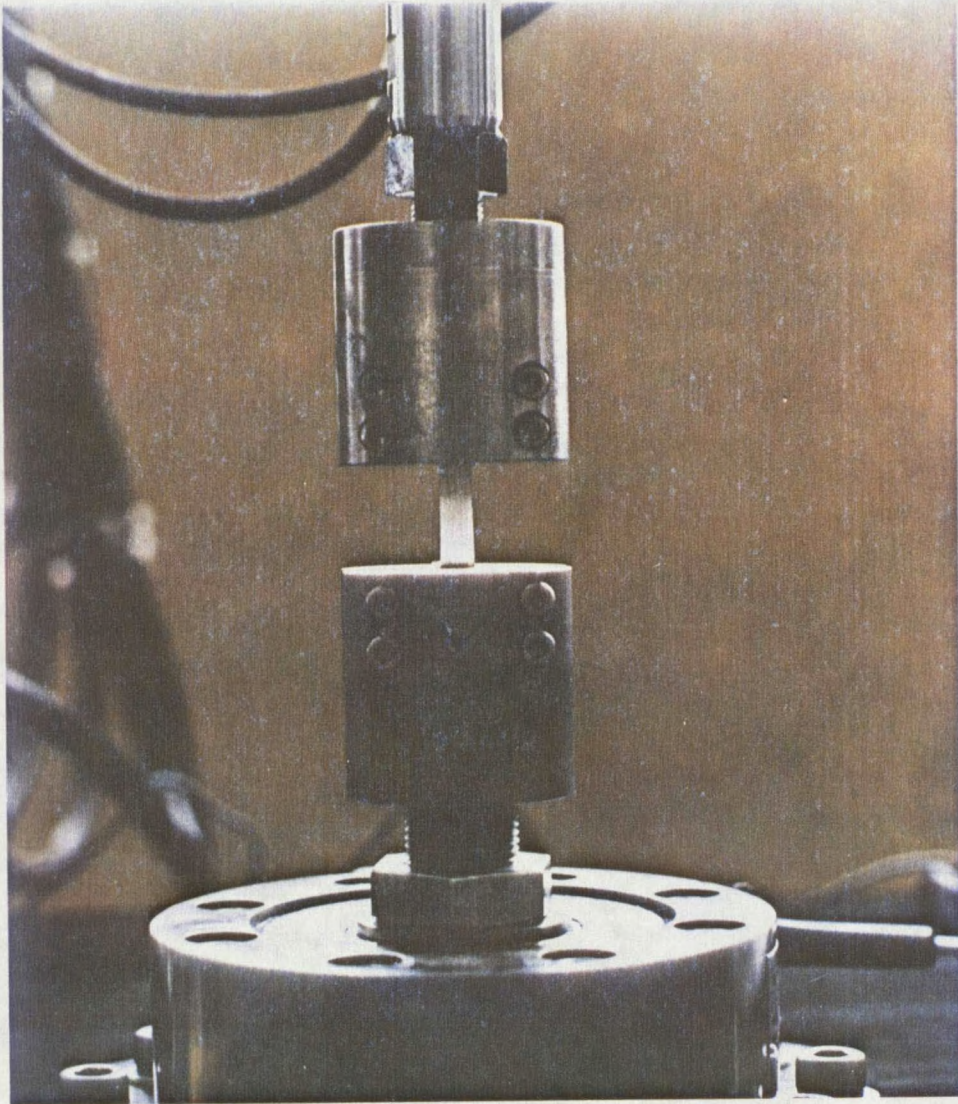


Figure 25. Photograph of grips with specimen running.

MONTANA STATE UNIVERSITY LIBRARIES



3 1762 10063631 3